

**LABORATORY INVESTIGATION OF NANO-  
ASSISTED POLYMER SOLUTION FOR EOR  
APPLICATIONS IN CARBONATE RESERVOIRS**

by

MEDET ZHANGALIYEV

2021

Thesis submitted to the School of Mining and Geosciences of Nazarbayev  
University in Partial Fulfillment of the Requirements for the Degree of  
**Master of Science in Petroleum Engineering**

**Nazarbayev University  
2021**

## **Acknowledgments**

I would like to express appreciation to thesis supervisor **Muhammad Rehan Hashmet** and to co-supervisor **Peyman Pourafshary** who gave me the chance to do the research project. The weekly meetings with supervisors were useful for guidance and motivation during such an unusual time as a pandemic period.

I would also like to extend my gratitude to **School of Mining and Geosciences** for providing with all the facility that was required.

Last but not least, I would like to give my special thanks to **my family and friends** for their unlimited support and love.

## **Originality Statement**

I, Medet Zangaliyev, hereby declare that this submission is my own work and to the best of my knowledge it contains no materials previously published or written by another person, or substantial proportions of material which have been accepted for the award of any other degree or diploma at Nazarbayev University or any other educational institution, except where due acknowledgement is made in the thesis.

Any contribution made to the research by others, with whom I have worked at NU or elsewhere is explicitly acknowledged in the thesis.

I also declare that the intellectual content of this thesis is the product of my own work, except to the extent that assistance from others in the project's design and conception or in style, presentation and linguistic expression is acknowledged.

Signed on **DATE**

---

## ABSTRACT

Currently, there have been a surge in evaluating effectiveness of various hybrid enhanced oil recovery (EOR) methods as it combines benefits of standalone processes. This study focuses on laboratory investigation to evaluate synergy between polymer and nanoparticles (NP), as their combination can alter capillary and viscous forces simultaneously.

N-vinyl-pyrrolidone based partially hydrolyzed polyacrylamide and silica oxide nanoparticles are used in this study. The standalone polymer, nanofluid (NF), and combined polymer-nanofluid solutions are prepared in different salinities (1200-40,000 ppm). The zeta potential of solutions is measured to determine the stability of NF at various salinities. Contact angle measurements are performed to screen the optimum concentration of NP. A series of rheological experiments are accomplished at different nanoparticle concentrations (0.05, 0.1, 0.15 wt%), temperatures (25-80 °C), and polymer concentration (500 to 3000 ppm). Additionally, a long-term stability test was also conducted for over thirty days at 80°C on nano-assisted-polymer fluid over a long period.

Zeta potential results proved that the stability of nanofluids decreases with increase in solution salinity. However, addition of polymer has positive impact on the stability of NF and are stable up to 40 000 ppm salinity. The nanoparticles have shown potential in altering wettability of rock towards the intermediate wet conditions. Maximum deviation of 55° in contact angle is noted for 0.1 wt% NP solution and is selected as optimum concentration. Rheology studies illustrate that the addition of NP increases viscosity of polymer solution by 25%. All nano-assisted-polymer solutions tested in this study showed shear thinning behavior. Long term thermal stability of nano-assisted-polymer solution indicates that the solution achieves equilibrium after 5 days and maintains target viscosity of 5 cP.

The addition of polymer has positively impacted on the salinity tolerance of nanoparticles. Additionally, nanoparticles improved viscosity of polymer solution. This study will open new doors for hybrid EOR method.

# Table of Contents

<b>TABLE OF CONTENTS.....</b>	<b>V</b>
<b>ABBREVIATIONS .....</b>	<b>VII</b>
<b>SYMBOLS .....</b>	<b>VII</b>
<b>LIST OF FIGURES .....</b>	<b>VIII</b>
<b>LIST OF TABLES .....</b>	<b>X</b>
<b>1. INTRODUCTION.....</b>	<b>11</b>
<b>1.1 Background.....</b>	<b>11</b>
<b>1.2 Problem definition.....</b>	<b>14</b>
<b>1.3 Objectives of the thesis.....</b>	<b>15</b>
1.3.1 Main objectives .....	15
1.3.2 Thesis structure .....	15
<b>2. LITERATURE REVIEW.....</b>	<b>16</b>
<b>2.1 Nanofluid aided polymer flooding .....</b>	<b>16</b>
<b>2.2 Polymer flooding .....</b>	<b>17</b>
2.2.1 Polymer properties at bulk conditions.....	17
2.2.2 Polymer performance in a porous media.....	21
<b>2.3 Nanofluids .....</b>	<b>24</b>
<b>2.4 Experimental studies of nano-assisted polymer flooding .....</b>	<b>31</b>
<b>3. METHODOLOGY .....</b>	<b>37</b>
<b>3.1 Materials .....</b>	<b>38</b>
3.1.1 Carbonate core.....	38
3.1.2 Formation water .....	38
3.1.3 Polymer .....	39
3.1.4 Nanofluid.....	39
<b>3.2 Procedure .....</b>	<b>40</b>
3.2.1 Fluid preparation .....	40
3.2.2 Contact angle measurements .....	41
3.2.3 Zeta potential tests.....	42
3.2.4 Rheology experiments .....	43
3.2.5 Long-term stability tests.....	45
3.2.6 Static adsorption analysis .....	45
<b>4. RESULTS.....</b>	<b>47</b>
<b>4.1 Contact angle measurements.....</b>	<b>48</b>

4.2 Zeta potential tests .....	51
4.3 Rheology experiments .....	54
4.4 Long-term stability tests .....	60
4.5 Static adsorption analysis .....	62
5. CONCLUSIONS AND RECOMMENDATIONS .....	65
6. REFERENCES .....	66

## ABBREVIATIONS

<b>ABS</b>	Absorbance
<b>ASP</b>	Alkaline Surfactant Polymer
<b>CPT</b>	Cloud Point Temperature
<b>EOR</b>	Enhance Oil Recovery
<b>FCM</b>	First Contact Miscibility
<b>MCM</b>	Multiple Contact Miscibility
<b>IEA</b>	International Energy Agency
<b>IFT</b>	Interfacial Tension
<b>IPV</b>	Inaccessible Pore Volume
<b>IOR</b>	Improved Oil Recovery
<b>HPAM</b>	Hydrolyzed Polyacrylamide
<b>NF</b>	Nanofluid
<b>NP</b>	Nanoparticle
<b>NPS</b>	Nano-assisted Polymer Solution
<b>PV</b>	Pore Volume
<b>RF</b>	Recovery Factor
<b>SP</b>	Surfactant Polymer

## SYMBOLS

$\alpha$	Contact angle
$\zeta$	Zeta potential
$\mu$	Viscosity
$t$	Time
$T$	Temperature

## List of Figures

Figure 1. Oil-recovery classifications (Adapted from Fundamentals of Enhanced Oil Recovery by Larry W.Lake) .....	11
Figure 2. Number of EOR projects in operation globally, 1971-2017 (Retrieved from official site of International Energy Agency) .....	12
Figure 3. The planning and structure of the thesis .....	16
Figure 4. The difference between a) waterflooding and b) polymer injection (Xia, et al., 2020).....	17
Figure 5. The structure of HPAM (Retrieved from Modern Chemical Enhanced Oil Recovery by Sheng J.) .....	18
Figure 6. The structure of Xanthan gum (Adapted from Modern Chemical Enhanced Oil Recovery by Sheng J.) .....	18
Figure 7. The reduction of three different polymer viscosity with increasing water salinity (Niu yabin, February 2001) .....	19
Figure 8. The influence of salinity to polymer at different degree of hydrolysis (H.Doe, May 1987) ..	20
Figure 9. The concentration of polyacrylamide and salt as a function of pore volume injected (Dawson, October 1972) .....	22
Figure 10. Viscosity as a function of temperature and long-term stability test (Ke Liang, 2019) .....	24
Figure 11. Wettability alteration of carbonate plate with various concentration of SiO <sub>2</sub> nanofluid (Abbas Roustaei, 17 August 2014) .....	26
Figure 12. IFT reduction with increasing concentration of nanofluids (Ragab, October 2015) .....	27
Figure 13. Viscosity of a heavy oil and a heavy oil with Al <sub>2</sub> O <sub>3</sub> nanofluid (Nares H.R., 2007) .....	27
Figure 14. Recovery factor of different nanofluids (Ogolo N.A., April 2012) .....	28
Figure 15. Recovery of oil by methal oxide nanoparticles after water flooding (Bayat E., September 2014) .....	29
Figure 16. Recovery factors of waterflooding and mixture of nanofluids (Alomair O.A., August 2015) .....	30
Figure 17. Impact of temperature on viscosity and on IFT of different solutions (Tushar Sharma, November 2016) .....	32
Figure 18. Recovery of factor and fractional flow versus time for different cases (Druetta P., 2019, February) .....	33
Figure 19. Rheological behaviour of polymer solution at different concentration of nanoparticles (Yadav U.S., 31 July 2019) .....	34
Figure 20. Emulsification between heavy oil and silica nanofluid aided xanthan gum polymer solution at different concentrations (Rahul Saha, 20 April 2018) .....	36
Figure 21. The chemical structure of HPAM-based polymer (Sheng, 2011) .....	39
Figure 22. Ultrasonic Homogenizer .....	41
Figure 23. OCA 15EC .....	42
Figure 24. Zetasizer Nano ZS .....	43



Figure 25. Anton Paar MCR 301 .....	44
Figure 26. The flow chart of the experiments .....	45
Figure 27. The relationship between absorbance and silica nanoparticle concentration.....	46
Figure 28. Adsorption calculation.....	46
Figure 29. UV Spectrophotometer .....	46
Figure 30. Contact angle difference vs. silica nanoparticle concentration.....	48
Figure 31. Contact angle measurements of 0.05, 0.1 and 0.15 wt%. .....	50
Figure 32. Illustration of zeta potential definition (NanoComposix, 2020) .....	51
Figure 33. The relationship of stability nano-assisted polymer solutions with increasing polymer concentration .....	53
Figure 34. SAV 10 rheology with increasing concentration .....	55
Figure 35. Rheology of SAV 10 with increasing temperature.....	55
Figure 36. The reduction of SAV 10 viscosity with increasing salinity .....	56
Figure 37. Rheology of nano-assisted polymer fluids with increasing concentration of silica nanoparticle.....	57
Figure 38. Effect of silica nanoparticle on viscosity of SAV 10 polymer solution .....	57
Figure 39. Rheology of nano-assisted polymer solutions with different concentration of polymer.....	58
Figure 40. Comparison of solutions .....	59
Figure 41. Rheology of 0.1 wt% silica nano-assisted 2000 ppm polymer solution with varying temperature .....	59
Figure 42. Long-term stability test of nano-assisted polymer solution .....	61
Figure 43. Thermal degradation factor of nano-assisted polymer solution.....	61
Figure 44. Long-term zeta potential test of nano-assisted polymer solution.....	62
Figure 45. Absorbance of nano-assisted polymer fluids with increasing concentration of silica nanoparticle.....	63
Figure 46. Corrected calibration curve .....	63
Figure 47. Comparison of two fluid absorbance .....	64

## List of Tables

Table 1. Ionizing compounds .....	38
Table 2. Composition of ions for 40 000 ppm brine .....	39
Table 3. The characteristics of nanoparticles.....	<b>Ошибка! Закладка не определена.</b>
Table 4. Results of contact angle measurements .....	49
Table 5. Zeta potential results of 0.05 wt% silica nanofluid with increasing salinity.....	52

# 1. Introduction

## 1.1 Background

The reservoir generally consists of the three phases of production. Primary recovery is the first stage of production where hydrocarbons are produced by primary reservoir drive mechanisms. On average, primary recovery can produce about 10 to 20% of the original oil in place (Green & Paul Willhite, n.d.). However, the recovery factor after primary production depends on the type of drive mechanism. The least efficient is compaction with 2-5% oil RF, while gravity drainage and water drives have the highest oil recovery range from 30% to 70%. After oil production is decreased by natural depletion, secondary recovery processes are used (Ahmed, 2010).

Secondary production is the second stage of oil recovery where immiscible water or gas are injected after natural depletion. The secondary recovery usually employs injecting water into the oil and gas reservoir which will maintain the reservoir pressure to produce more oil out of the reservoir. On average, secondary recovery can produce another 10 to 20% of the original oil in place (Green & Paul Willhite, n.d.).

The next stage is tertiary production widely known as enhanced oil recovery (EOR). These methods could change rock and fluid properties. EOR consists of thermal methods, chemical injection, solvent injection methods (Larry W.Lake, 2014). Three stages of oil production are presented in Figure 1.

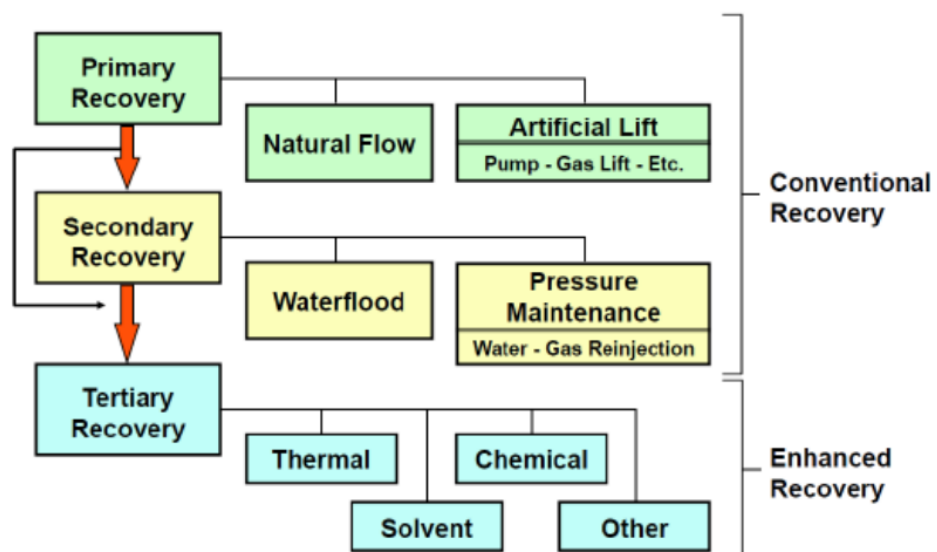


Figure 1. Oil-recovery classifications (Adapted from Fundamentals of Enhanced Oil Recovery by Larry W.Lake)

Enhanced oil recovery is the process of injecting a non-reservoir fluid into the reservoir. The main objective of an EOR process is to reduce residual oil saturation from existing fields by changing capillary and viscous forces. Currently, the petroleum industry reached a point when the potential for enhanced oil recovery from existing resources exceeds the potential from discoveries (Larry W.Lake, 2014).

Based on rock and fluid characteristics, three main EOR techniques exists, which are thermal methods, chemical injection, miscible gas, and solvent injection methods. According to International Energy Agency (IEA), thermal methods have the highest number of EOR projects worldwide while other methods including foam, microbial injections are less frequently used. Overall, over 400 chemical projects and 800 carbon dioxide EOR methods are operated globally from 1971 and 2017 years as illustrated in Figure 2.

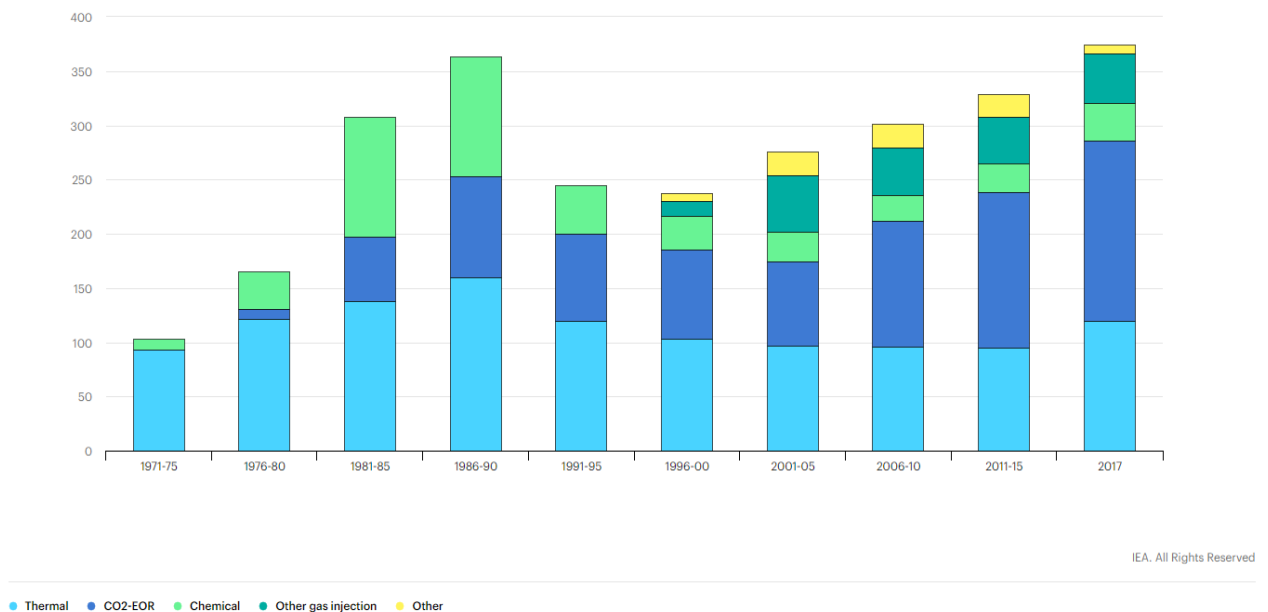


Figure 2. Number of EOR projects in operation globally, 1971-2017 (Retrieved from official site of International Energy Agency)

The thermal EOR method is applied in bitumen and tar sand reservoirs as a primary or secondary stage. Since heavy oil reserves are not movable, it must be heated to make heavy hydrocarbons flow. Steam injection, steam-assisted gravity drainage, in-situ combustion, and cyclic steam stimulation are the types of thermal methods. This technique lowers the viscosity of oil with increasing temperature. Since oil becomes more mobile it produces more than initially (Lim K.T., 1992) Thermal methods are the most widely used technique because 2/3 of reserves are heavy oil reservoirs. However, the applicability of steam injection methods differs from in situ combustion techniques. Steam can not be injected in deep, high-pressure, and low

permeability reservoirs due to heat loss and insufficient usage as well. On the other hand, in situ combustion is suitable for deep reservoirs and can be used for maintaining reservoir pressure (Green & Paul Willhite, n.d.).

Solvent flooding is the second widely used method of EOR. It includes carbon dioxide (CO<sub>2</sub>), nitrogen, flue gas, sour and sweet gas injections (Green & Paul Willhite, n.d.). Increasing incremental oil recovery during solvent injection is driven by changing the composition and phase of the crude oil. The working principle can be described in macroscopic and in microscopic scales. Microscopic sweep efficiency is affected by the type of miscibility of solvents in the crude oil. At first contact miscibility (FCM), solvents directly mix with oil, while at multiple contact miscibility (MCM), miscible solution forms later. The type of miscibility depends on injection pressure and the composition of solvents. The optimal conditions for first contact miscibility are similar composition of solvents related to the crude oil and injection pressure should be higher than minimum miscibility pressure. Macroscopic sweep efficiency is sensitive to reservoir heterogeneity and gravity. Since gas is less dense than formation fluid, it tends to segregate bypassing a significant amount of oil. Water alternating gas (WAG), reducing the distance between wells, and lowering perforation level are proposed solutions to avoid issues such as early gas breakthrough and gravity segregation.

Chemical injection is one of the trending methods for enhancing oil recovery because water floods alone usually do not achieve a uniform sweep through heterogeneous reservoir rock. The types of chemical EOR includes polymer, surfactant, alkaline, polymer surfactant (SP), alkaline surfactant polymer (ASP) injection (Green & Paul Willhite, n.d.). The drive mechanisms of polymers, surfactants and alkaline are different. Polymer increases viscosity of displacing fluid. “Fingering” effect is prevented, and injection process will be a more piston-like displacement during polymer flooding. Therefore, improves volumetric sweep efficiency. As less oil is captured during water injection into the reservoir, surface active agents are added. The surfactant is mixed with water and flooded into a reservoir. It reduces the interfacial tension between oil and water and thus decreases residual oil saturation, thereby improving microscopic sweep efficiency. In addition to surfactant flooding, in some cases use of alkali enhances surfactant performance. Alkalines form surfactants inside reservoir rock by reaction with acidic components of oil to remove remaining oil by lowering IFT. The variation of surfactant polymers (SP) or alkaline surfactant polymers (ASP) are carried out to alter capillary and viscous forces.

Presently, modern physics proposes the utilization of nanotechnology as a new chemical EOR method. Several nanoparticles were invented where there are working principles that are different from each other. Thus, each nanoparticles have a particular drive mechanism (Ogolo N.A., April 2012). Details are written in further sections. However, the common characteristics of them are their nano size, cost-effectiveness, and environmentally friendly substances. These general qualities make nanotechnology an appealing method to implement as one of the tertiary stages of oil recovery (Xiaofei Sun, February 2017). Various experiments were conducted to raise the efficiency of nanoparticles. One of them was the combination of nanoparticles and polymer flooding. The idea behind this integration was to advance capillary and viscous forces by synergy between chemicals. Polymer improves viscous forces, while nanoparticles impact on capillary forces. Thus, combination of nanoparticle and polymer solutions present an attractive research topic.

## **1.2 Problem definition**

The prospective of increasing oil production from existing resources exceeds the potential from oil field discoveries at present. If the petroleum industry follows traditional management such as drilling and waterflooding, even sustaining production levels will be difficult or not imagine increasing recovery factors. Furthermore, if the industry does not introduce enhanced oil recovery methods, then amount of unrecoverably oil will be significant. Therefore, the oil and gas sector focuses on improving recovery factors with EOR technology. There are many EOR projects implemented over the years in sandstone and carbonate formations. According to forecasts, the market value for the EOR project in 2025 will be increased by 58.67 % compare with the 2018 year. It implies the attractiveness of EOR for investors (Sönnichsen, 2021). Therefore, new methods are invented every year. One of them is using nanoparticles as EOR technology. Since nanoparticles size is lesser than the average pore throat, it can flow through inaccessible pores. Thus, NPs cover more unswept zones due to size and high surface-to-volume ratio. This helps to cover a large surface area with fewer NPs numbers. Above mentioned parameters of nanoparticles, show the possibility to implement NPs in the petroleum industry. At the same time, the quality of available polymers is improving as they showed promising results as EOR technology. Polymer improves volumetric sweep efficiency by preventing the water from fingering through the oil. It also increases viscosity a displacing fluid that acts in a more piston-like displacement. Therefore, using polymers with nanofluids might advance the efficiency of flooding by changing the capillary and viscous

forces. However, the existing research is lacking in terms of its application in harsh conditions. This has not been conducted before because nano-assisted polymer flooding in high salinity and high temperature is relatively a new topic. Thus, this research is worth doing because of methodological limitations.

### **1.3 Objectives of the thesis**

#### **1.3.1 Main objectives**

The main target of the research is to integrate and assess nanoparticle and polymer flooding together to ensure improvement in the recovery mechanisms. The following shows clarification of the objective:

- To validate the efficiency of driving mechanisms of nanoparticle and polymer in their combination.
- To examine the stability of integration of nanofluids and polymers from ambient environment (25°C, 1200 ppm salinity) to reservoir conditions (80°C, 40,000 ppm salinity).
- To screen optimum concentrations of silica nanoparticle and modified synthetic polymer that can tolerate 40,000 ppm salinity, 80°C reservoir temperature conditions.

#### **1.3.2 Thesis structure**

The thesis structure was designed in reference to the main objective. Generally, the research is divided into three major sections namely methodology, results, conclusions, and recommendations. Each section is aimed to achieve the primary target of the thesis. Thus, they had subsections.

Methodology consists of materials and procedure sections. Materials subsection illustrates required resources for further actions. Formation water, polymer, nanofluid, and carbonate core sample were used as materials. Procedure subsection shows parts of the project and their working processes, including wettability alteration, stability tests, rheology of fluids, long-term stability, and static adsorption analysis.

Results involve the data and discussion from experiments. These sections were constructed in a such way as to examine the combination of nanofluids and polymers in various conditions. The subsections are contact angle measurements, zeta potential tests, rheology of solutions, long-term stability, and static adsorption analysis. The contact angle measurements

and zeta potential tests were used to screen the most effective nanofluid for further experiments. On the other hand, the rheology experiments were utilized to select the optimum concentration of modified synthetic polymer with the screened concentration of nanoparticles. The remaining two experiments, long-term stability test, and static adsorption analysis demonstrate results of the screened concentrations of nano-assisted polymer solution. More details and discussion were indicated in the subsections.

The conclusion and recommendation section highlights the key points of the combination of nanoparticle and polymer flooding for EOR purposes study. There are no subsections. The recommendations were written for advanced research in particular performing core flooding experiments and designing smart injection techniques with the selected concentration of nano-assisted polymer solution.

Figure 3 displays the schedule to complete each subsection and organizational parts of the thesis. Overall, it took 1 year to finish the thesis where each subsection was performed roughly a month to generate high-quality results. There is additional information that demonstrates the planning and structure of the thesis.

Year	2020								2021			
Months	May	June	July	August	September	October	November	December	January	February	March	April
Activities												
Study Nanoparticles												
Study Polymer flooding												
Writing the Literature Review												
The Methodology Preparation												
Fluids preparation												
Performing zeta potential tests, contact angle measurements												
Rheological experiments												
Long-term stability tests, static adsorption measurements												
Thesis Writing												
Thesis Defence												

Figure 3. The planning and structure of the thesis

## 2. Literature Review

### 2.1 Nanofluid aided polymer flooding

The increased oil production due to the combination between polymers and nanoparticles were reported by laboratory experiments ( (Maghzi A., February 2014), (Cheraghian, 25 May 2016), (Tushar Sharma, November 2016), (Laura Corredor, October 2018), (Karl, January 2019)). Polymer floods accelerated the production of oil by reducing



mobility ratio ( (Duda L., October 1981), (Argabright A., 1982), (DeHekker G., 1986), (Wang D., 2000)). On the other hand, nanoparticles showed essential characteristics such as wettability alteration, lowering interfacial tension, and decreasing the viscosity of crude oil, which affects on reduction of residual oil saturation ( (Ogolo N.A., April 2012), (Bayat E., September 2014), (Alomair O.A., August 2015), (Tarek, September 2015), (Hu Z., March 2016)). Therefore, using polymers with nano-fluids might advance the efficiency of flooding by changing the capillary and viscous forces.

## 2.2 Polymer flooding

Polymer flooding is a commercial project, where the quality of polymers is advancing, as they showed promising results as chemical IOR technique. Polymer improves the mobility ratio by increasing the viscosity of injecting fluid, which is usually water. It implies significantly better volumetric sweep efficiency than water flooding because polymer injection prevents the fingering effect, as shown in Figure 4. On the other hand, polymers do not change residual oil saturation.

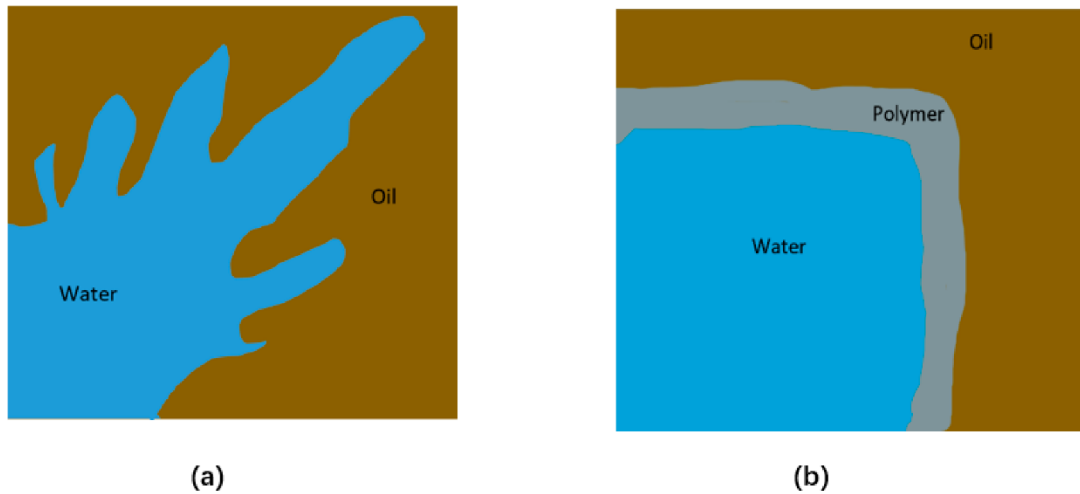


Figure 4. The difference between a) waterflooding and b) polymer injection (Xia, *et al.*, 2020)

Normally, there are two types of parameters that we need to consider. One of them polymer have to be examined as a bulk material. Another one is polymer performance in a porous media.

### 2.2.1 Polymer properties at bulk conditions

Polymers are macromolecules consisting of repeating monomers (Gad, 2014). They are divided into two main groups, which are synthetic polymers and biopolymers. Synthetic polymers consist of acrylamide monomers. They are partially hydrolyzed also known as

partially hydrolyzed acrylamide (HPAM). A commonly used biopolymer is xanthan gum (Larry W.Lake, 2014).

HPAM is a widely used hydrolyzed synthetic polymer which consists of acrylamide groups ( $CONH_2$ ) and from negatively charged carboxyl groups ( $COO^-$ ) at edges of polymer structure. The chemical structure of HPAM is presented in Figure 5. The idea of making it hydrolyze is to replace some amount of amides with carboxyl groups. The carboxyl group stretches the polymer chains, which allows to have high viscosity. Subsequently, the stability of HPAM will reduce with increasing number of carboxyl groups. The stability of HPAM depends on the number of acrylamide groups. Additionally, there are inexpensive and resistive to bacteria (Sheng, 2011).

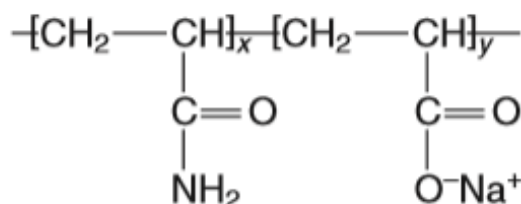


Figure 5. The structure of HPAM (Retrieved from Modern Chemical Enhanced Oil Recovery by Sheng J.)

Xanthan gum is a biopolymer that consists of the base molecule of saccharide structure. At the same concentration of polymers, the viscosity of xanthan gum is lower than HPAM. However, biopolymers can withstand degradation at relatively high temperatures ( $<80^\circ\text{C}$ ) than synthetic polymers, as shown in Figure 6 (Kierulf C., 1988) (Sheng, 2011).

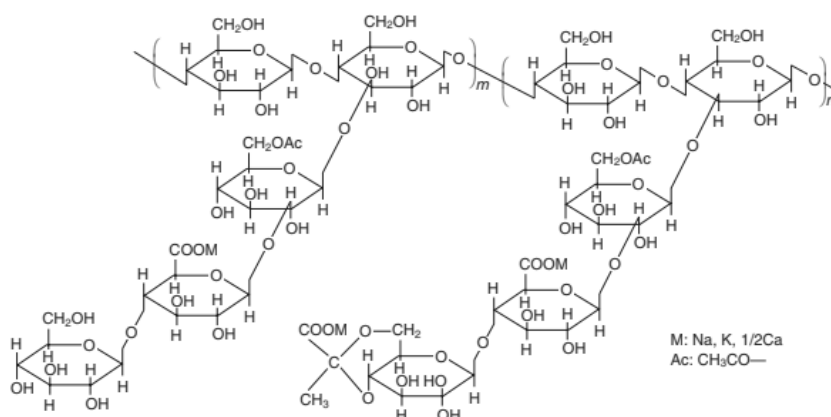


Figure 6. The structure of Xanthan gum (Adapted from Modern Chemical Enhanced Oil Recovery by Sheng J.)

There are various types of polymers. One of them is applicable for high temperature, high salinity conditions whereas usage of others are completely at different environment.

Therefore, it is critical to consider the rheology of polymers in various states. In our case high salinity, high temperature referred as harsh conditions. The first parameter which is impact viscosity is the stability of the polymer. Polymer chains have to remain its structure inside formation. If for any reason, the long molecule structure of polymer breaks, so it will mean that polymer does not work. This might happen at high pressure, applied mechanical force, or high salinity. In presence of high salinity brine, positive cations of brine ( $Na^{2+}$ ,  $Ca^{2+}$ ,  $Mg^{2+}$  and etc) will replace negatively charged anions of polymer. Since positive and negative ions attract to each other, polymer structure will be “coiled” (H.Doe, May 1987). The idea of evaluating the stability of polymers is to measure viscosity at different temperatures or at different times. Thus, it is critical to consider the rheology of polymer. Polymer rheology is impacted by the molecular weight of polymer, polymer concentration, water salinity, shear-thinning behavior.

Niu Yabin experimented with the impact of brine on the rheology of synthetic polymers, such as HPAM and hydrophobic polymers. The obtained results show the general behavior of polymer to salinity. When salinity increases from 1000 g/L to 7000 g/L, polymer viscosity decreases for all concentrations, as illustrated in Figure 7 (Niu yabin, February 2001).

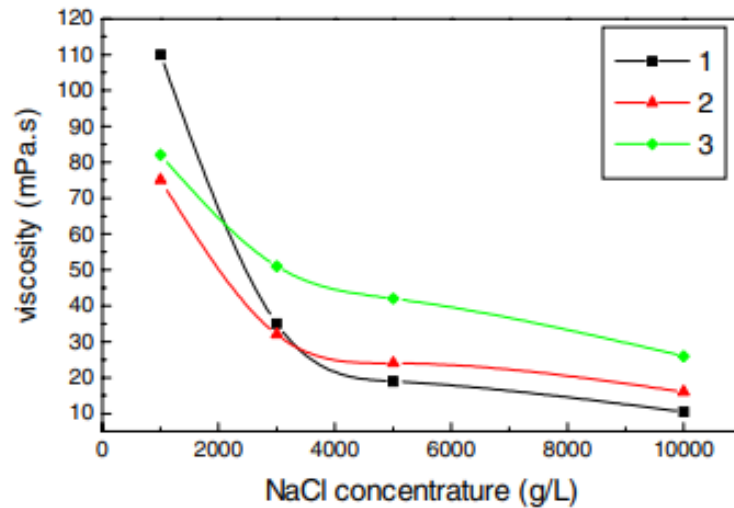


Figure 7. The reduction of three different polymer viscosity with increasing water salinity (Niu yabin, February 2001)

Moradi-Araghi and Doe investigated the influence of salinity on polymer at different degrees of hydrolysis. As an overview, the stability of polymer becomes weaker with increasing salinity as there is more chance of “coiling”. If polymer hydrolyzation in water is at a high extend, the process of “coiling” will happen more. “Coiled” structure significantly affects on

properties of polymer. The effects are reduction of viscosity and stability because when polymer is coiled there is more chance for precipitation. The numerical parameter, that defines stability, is cloud point temperature (CPT). At this temperature, the polymer starts to separate from water. If CPT is at a lower degree, the stability will be reduced. In Figure 8, two parameters are shown. On the horizontal axis is the concentration of cations and different curves of various degrees of hydrolysis. As mentioned, the stability of polymer becomes weaker with increasing salinity as there is more chance of “coiling”. For instance, polymer is stable up to 200°C at low salinity but at high salinity, the stability occurs up to room temperature. Noticeably, all polymers behave similarly at low salinity. Thus, there is no problem of “coiling” at low salinity. However, the challenges happens at high salinity (H.Doe, May 1987).

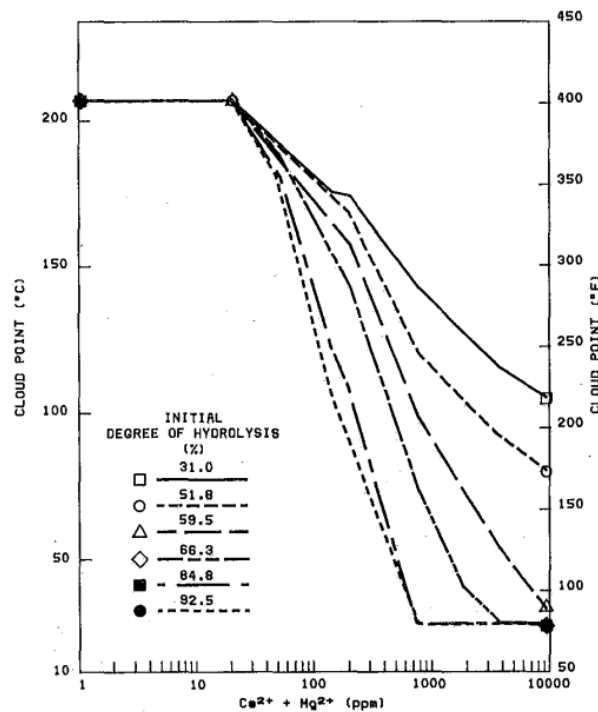


Figure 8. The influence of salinity to polymer at different degree of hydrolysis (H.Doe, May 1987)

One important parameter that impacts the stability of the polymer is the shear rate. Generally, the viscosity of the polymer decreases at a higher shear rate. This is called shear thinning, which means polymer becomes thinner by shear. At a low shear rate, the behavior is Newtonian. While at a very high shear rate polymers acts as water. It does not have any effect on viscosity. Carreau tried to model the dependence of viscosity fluid to shear rate. He assumed that the viscosity of the polymer is zero at higher shear rate, whereas the viscosity of polymer is infinity at lower shear rate. These two parameters are constant. The proposed model explains the shear-thinning behavior of polymer but in dimensionless form (Carreau, 1972). There are

other models similar to Carreau's, for instance, Tsaur proposed the model for different concentrations of polymer for higher shear rate. The reason for constructing this model is applicability, as for lower shear rate all polymers are the same, while for higher shear rate they are different (Tsaur, December 1979).

The next essential parameter is temperature. Normally, temperature exponentially decreases the viscosity of the polymer. Noticeably, the behavior of polymer might be different at room temperature than at reservoir temperature. Another effect is pH. A similar pattern can be noticed with the effect of salinity. When pH changes, the charge of molecules alters. Thus, for different pH viscosity changes and type of oil have to be considered carefully. For low and high pH, the viscosity is low.

### **2.2.2 Polymer performance in a porous media**

In the porous media, other parameters are crucial. For example, there is adsorption of polymer on rock surface or polymer flows to different pores at heterogeneous reservoirs. All of these items are not considered in bulk conditions. Therefore, in the porous media polymer viscosity, polymer retention, inaccessible pore volume, and permeability reduction have to be examined. For example, polymer viscosity changes in the reservoir because the forces applying to the polymer are different in the reservoir. The shear will be higher in small pores than in bigger pores. Thus, more chances of changing viscosity.

Polymer retention is a critical parameter, which depends on adsorption and mechanical entrapment mechanisms. In the case of polymer adsorption, the cost of flooding will be high because more polymer is required with increasing polymer retention. Polymer adsorption happens due to different charges between polymer and rock surfaces that attach to each other. Thus, the degree of adsorption is different for various rocks. For example, for sandstone isoelectric point or known as IEP, the point where pH is not positive or not negative, is at pH equal to 2, but for carbonate, it goes around 9 for different kinds of carbonate formations. It means that at normal conditions at pH=7, sandstone charge is negative, while carbonate charge is positive (Jaafa M.Z.r, 2014). Therefore, if we won't use anionic polymer, there will be more chance of adsorption on carbonate rock. On the other hand, mechanical entrapment is one of the mechanisms of polymer retention that occurs due to permeability reduction. Adsorption and mechanical entrapment makes retention. Various papers tried to model polymer retention. These models take into account the concentration of polymer and constant reservoir conditions.

Normally, If there is a high concentration of polymer, adsorption will be higher. Noticeably, the unit of adsorption is the mass of polymer adsorb on 1 gram of a unit mass of a rock.

A similar situation can be noticed with inaccessible pore volume or known as IPV. If the pores are small, the polymer will not flow in that pores because molecules are longer. For instance, injected water flows everywhere, but some parts are inaccessible for polymer flooding. Dawson and Lantz investigated the effect of IPV on polymer and saltwater performance. They found that polymer breakthrough is sooner than saltwater. Figure 9 shows the concentration of the effluent to fluid injection pore volume. Polyacrylamide breakthrough is earlier compare to saltwater. From Figure 9, the percentage of inaccessible pore volume is estimated by the difference of the fronts of two fluids. As a result, IPV is about 24 % (Dawson, October 1972). If the IPV value is significant, the selected polymer will not be applied to this field, because it will flow to a minor portion of the reservoir and most of the pores are not accessible.

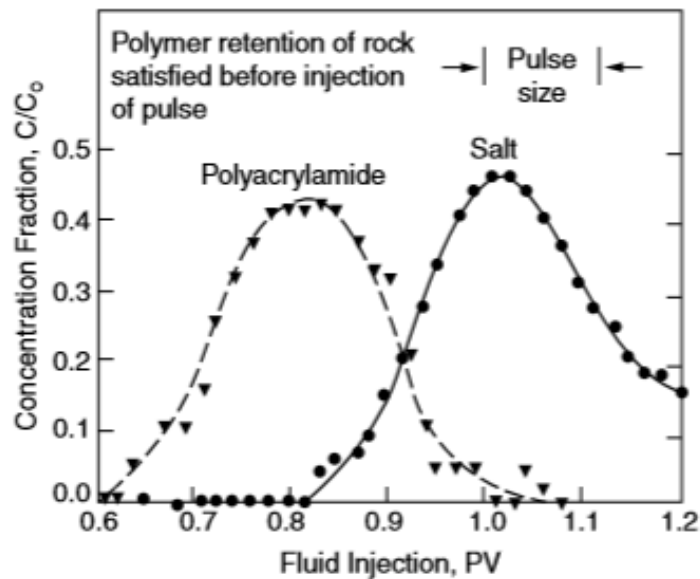


Figure 9. The concentration of polyacrylamide and salt as a function of pore volume injected (Dawson, October 1972)

Huges experimented with polymer and brine (tracer) flooding, to estimate IPV and retention. The first polymer slug was injected at the same time followed by brine flooding then the second polymer slug was injected into a core sample. The result was the cumulative fraction of concentration that is received. Retention is found by the difference between the first and second slugs of polymers. Since the first slug flows in any place it can go the second slug shows

polymer after that. While the difference between brine and first slug represents IPV (Huges, February 1990).

Another significant parameter that impacts the effectiveness of polymer flooding in porous media is called mechanical degradation. Since the rate of polymer injection is high near-wellbore the long structured polymer breaks. After that, there will be smaller molecules in the system. For this reason, the viscosity will be lower. Additionally, the effect is worse at lower permeability. Two parameters represent mechanical degradation. One of them is the resistance factor or RF. RF compares the viscosity of polymer and water that further shows the mobility of water and polymer. If RF is equal to 1, then the polymer will behave exactly as water. It implies that polymers are completely lost. The other one is the residual resistance factor or RRF. RRF compares mobility of water before and after polymer injection. It indicates the remaining polymer flooding. For example, If there is high retention, then most of the pores will be blocked. Consequently, mobility of before will be much greater than mobility of after polymer injection (Needham R.B., 1974).

$$RF = \frac{\mu_p}{\mu_w}; \quad RRF = \frac{\lambda_{w1}}{\lambda_{w2}}$$

An alternative method that reflects mechanical degradation is screen factor or SF. SF compares the flow time of the volume of polymer solution and flow time of volume of water. In other words, the screen factor compares the viscosity when the fluid is in motion. When SF is high, it implies that the polymer is excellent.

The parameters such as salinity, temperature, and type of rock are those main properties that set screening criteria for polymers. HPAM and xanthan gum are not suitable at harsh conditions such as high temperature ( $> 80^{\circ}\text{C}$ ) and high salinity because the viscosity will be reduced and polymer chains will break down respectively. Therefore, synthetic co-polymers and new biopolymers have to be chosen considering stability in saline environment and rheological properties as a function of temperature.

Muhammad Hashmet investigated polymer performance at high temperature, high salinity carbonate reservoir. He conducted a core flooding test with X-ray records. Then the data was matched with the simulation model to estimate optimum polymer size. The results show that the highest recovery of oil was achieved by 0.1PV polymer flooding, which was injected after 0.3 PV water flooding. Additionally, the author reported that modified polyacrylamide polymer, commercial name is SAV10, was stable long term in harsh conditions

(Muhammad Rehan Hashmet, April 2017). Therefore, modified polyacrylamide polymer SAV10 could be used for further studies. However, the size of the polymer should be small to minimize polymer retention as suggested by the researcher.

Lian and his colleagues compared the rheological properties of a synthetic polymer and biopolymers at high temperature and high salinity conditions. According to the information obtained, biopolymers such as xanthan gum, diutan gum, and scleroglucan are less dependent on temperature. Figure 10 presents the viscosity of polymers against temperature. As an overview, scleroglucan is less sensitive to temperature whereas HPAM is strongly controlled by heating. Noticeably, different concentrations of polymers (0.075wt% HPAM, 0.25wt% Xanthan gum, 0.25wt% Scleroglucan, 0.1wt% Diutan gum) were used to achieve the initial viscosity at ambient temperature. Furthermore, diutan and scleroglucan are stable in long terms while HPAM and xanthan gum showed viscosity reduction (Fig.5). Thus, biopolymers could be chosen for further applications (Ke Liang, 2019).

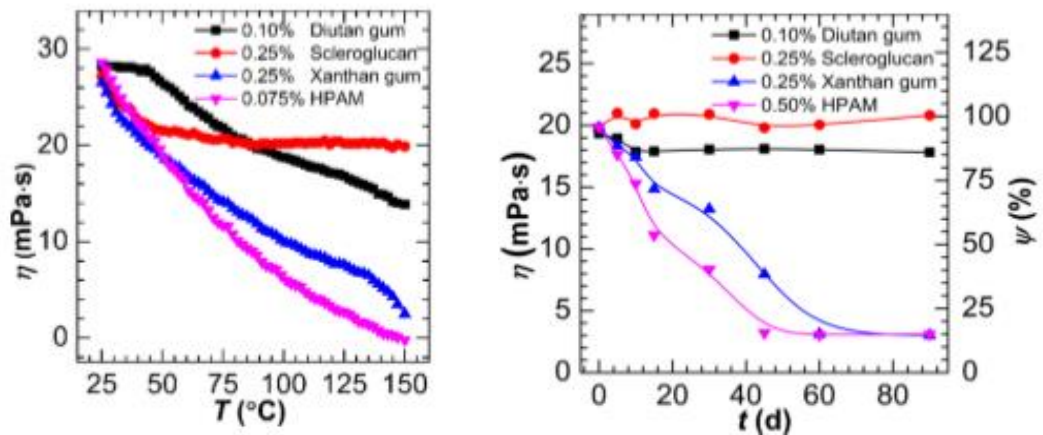


Figure 10. Viscosity as a function of temperature and long-term stability test (Ke Liang, 2019)

## 2.3 Nanofluids

There is increasing interest in nanoparticles because Krishnamoorti (2006) identified “it merges unique physical and chemical characteristics in the size range from 1 nm to 100 nm”. Since nanoparticles size is lesser than the average pore throat, it can flow through inaccessible pores. Thus, NPs cover more unswept zones due to size and high surface-to-volume ratio. This helps to cover a large surface area with fewer NPs numbers. Above mentioned parameters of nanoparticles, show the possibility to implement NPs in the petroleum industry. Particularly, widely employed nanoparticles, which are SiO<sub>2</sub>, TiO<sub>2</sub>, Al<sub>2</sub>O<sub>3</sub>, are already used to improve enhanced oil recovery methods (Xiaofei Sun, February 2017).



Nanoparticles or NPs are designed to serve as nanofluids, nanoemulsions, and nanocatalysts (Xiaofei Sun, February 2017). Nanofluids are frequently used while nanoemulsions and nanocatalysts are less analyzed.

Nanofluid is the solution of nanoparticles and fluids. Various nanofluids have different properties. Some of them change wettability, whereas others reduce interfacial tension IFT or decrease the viscosity of oil. Interestingly, the wettability alteration has been more deeply analyzed and proven than other properties of nanofluids. For example, Roustaei and Bagherzadeh investigated the influence of SiO<sub>2</sub> silicon oxide nanofluid on the wettability of a carbonate rock. They used oil-aged carbonate plates to measure contact angle. It shows that silica oxide nanofluid has the property to alter the wettability of carbonate rock towards strong water-wet. However, wettability alteration depends on concentration of injecting silicon oxide nanofluid. The optimum concentration should be equal or higher than 4 g/L. This property of SiO<sub>2</sub> nanofluid could significantly increase oil production from carbonate reservoirs, as shown in Figure 11 (Abbas Roustaei, 17 August 2014). Additionally, the wetting angles were measured between the dropping phase (oil) and rock surface. The right and left contact angles represent the measurements from both sides to obtain representative results. Noticeably, the ambient phase is formation water, and dropping phase is oil. Karimi conducted a similar experiment on wettability alteration of carbonate rock with ZrO<sub>2</sub> zirconium oxide nanoparticle. The contact angle was measured by side images after aging carbonate rock with oil. Results indicate that wettability of carbonate outcrop was changed from oil-wet to intermediate wet, then wettability was altered to strong water-wet with more addition of ZrO<sub>2</sub> zirconium oxide nanoparticle. At least 48 hours were required to alter the wettability of carbonate rock towards water-wet based on the outcomes of the experiment. Additionally, Karimi introduced mathematical model which clarify this characteristic of nanoparticle (Karimi A., January 2, 2012). However, the model could be improved by inserting several parameters such as interfacial tension IFT. Certainly, this property of nanofluid will improve EOR methods. Wasan explained the reason for changing wettability while using certain types of nanofluids. The researcher concluded that the wettability alteration is created due to the wedge-shaped film between rock-oil-water interactions in presence of nanofluids (Wasan D., March 11, 2011).

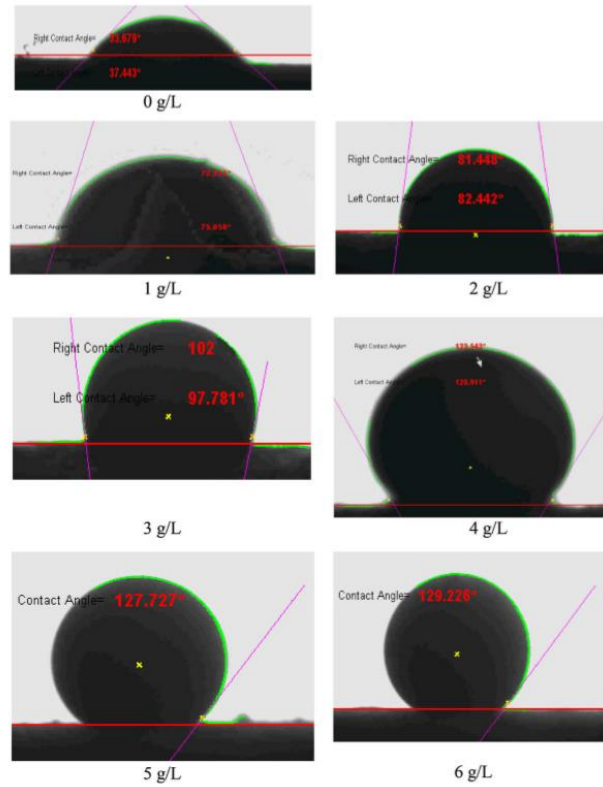


Figure 11. Wettability alteration of carbonate plate with various concentration of SiO<sub>2</sub> nanofluid (*Abbas Roustaei, 17 August 2014*)

The next essential property of nanofluid is the reduction of IFT. Ragab experimented on the impact of different concentrations of single silicon oxide and aluminum oxide (0.1, 0.5, and 1wt%) nanofluids on interfacial tension. IFT was measured by spinning drop video tensiometer at ambient and reservoir temperatures. The results represent that silica nanofluid affects more on reduction of IFT than alumina oxide nanofluid. Noticeably, in both cases, interfacial tension decreases with increasing concentration of nanofluids (Ragab, October 2015). Suleimanov studied the influence of nanofluids on the reduction of IFT. Interfacial tension was determined by a drop shape tensiometer. It shows that nanofluids decreased IFT to 70-90% (Suleimanov B.A., 6 June 2011). Zhang reported a significant decrease of interfacial tension from 16 mN/m from 1.4 mN/m between silica nanofluid and oil (Zhang H., April, 2014). However, Moradi with his colleagues observed a minor reduction of IFT from 13.62 mN/m to 10.69 mN/m between silica nanofluid and oil (Moradi B., November, 2015). These differences might occur due to the composition of base fluid or crude oil. Another reason might be the different procedures of both work. Noticeably, decreasing IFT was not a single mechanism while using nanofluids. It came with wettability alteration. This might happen due to the type

of nanoparticle. Despite that, residual oil saturation could be greatly minimized by injection of nanofluids due to IFT reduction as well.

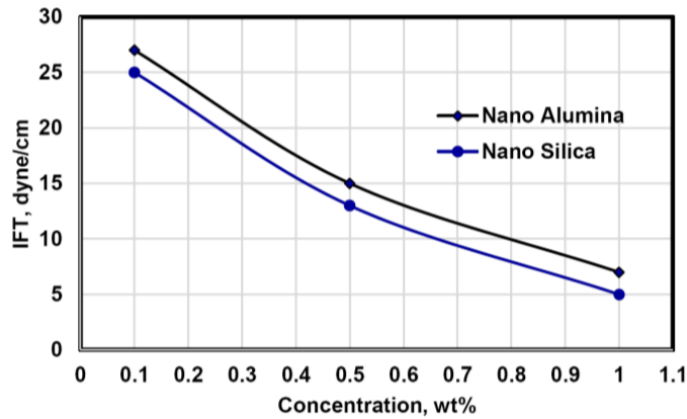


Figure 12. IFT reduction with increasing concentration of nanofluids (*Ragab, October 2015*)

Another important characteristic of nanofluid is the viscosity reduction of crude oil. Nares with colleagues studied the influence of aluminum oxide Nanofluid on the viscosity of a heavy oil. They compared the properties of pure heavy oil and modified a heavy oil with nanofluids. It is shown that  $\text{Al}_2\text{O}_3$  nanofluid reduces the viscosity of oil because heavy oil components are transformed to lower oil components, also known as the hydrocracking process. Additionally, aluminum oxide reduces the amount of sulfur and coke as well. Thus, this characteristic allows a heavy oil to be more mobile, as presented in Figure 13 (Nares H.R., 2007).

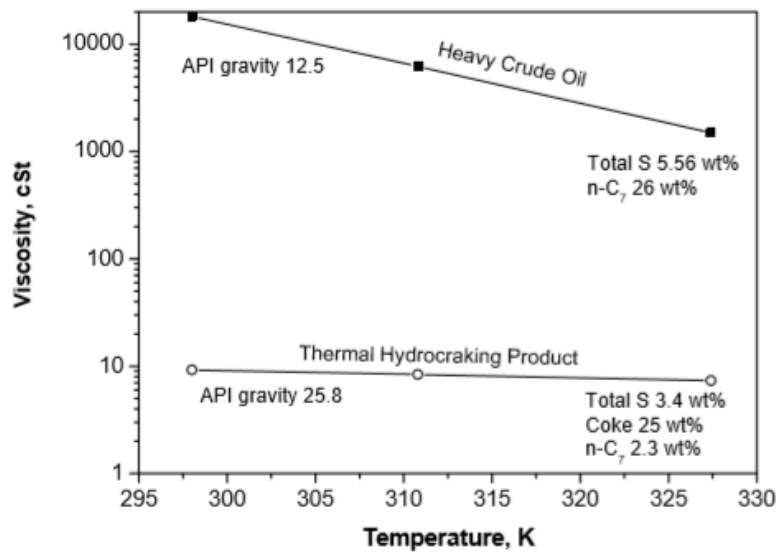


Figure 13. Viscosity of a heavy oil and a heavy oil with  $\text{Al}_2\text{O}_3$  nanofluid (*Nares H.R., 2007*)

Those properties of nanofluids increase oil production. Some researchers concluded that using nanofluids is effective for increasing incremental oil recovery. As an example, Ogolo showed that using nanoparticles in base fluids have a higher recovery factor of oil than using a single injected base fluids. This enhancement generally for Silicon oxide, Aluminium oxide nanoparticles in terms of oil recovery. This is due to the ability of Silicon oxide, Aluminium oxide to change wettability and to reduce viscosity of oil respectively. While Zinc oxide and Magnesium oxide reduces oil recovery as they tend to create permeability issues. The presence of nanoparticles in base fluids changes its properties and increases the effectiveness of flooding on oil recovery processes, as shown in Figure 14 (Ogolo N.A., April 2012). However, it should be noted that distilled water, ethanol can not be used as base fluids in reservoir conditions because in the worst-case scenario shale might be swelled.

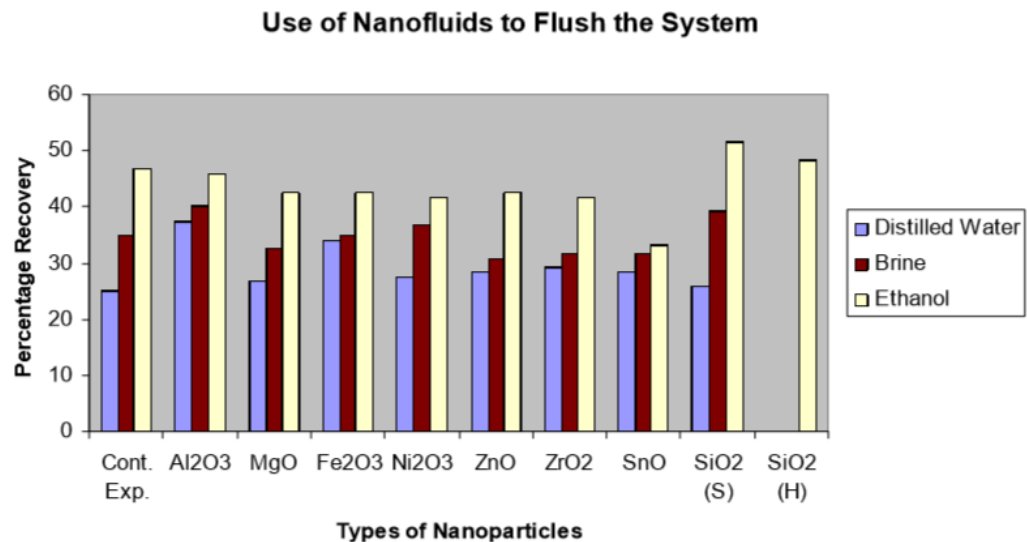


Figure 14. Recovery factor of different nanofluids (Ogolo N.A., April 2012)

Bayat investigated separately the influence of silica oxide, titanium oxide, and aluminum oxide nanoparticles on the recovery efficiency of oil. The researcher conducted a rheological test and core flooding. Additionally, all experiments were performed on limestone at several temperatures and nanoparticles were diluted in low-salinity water. Obtained outcomes show that the wettability of limestone altered towards water-wet because of the adsorption of nanoparticles. The highest adsorption shows SiO<sub>2</sub> silica oxide nanoparticles while the lowest adsorption was at Al<sub>2</sub>O<sub>3</sub> aluminum oxide nanoparticles. Moreover, a significant reduction of IFT was observed at all temperatures. Aluminum and titanium oxide affects more on IFT than silica oxide nanoparticles. As a result, the recovery factor of oil increased due to changes in capillary and viscous forces (Bayat E., September 2014).

Figure 15 demonstrates the recovery factor of oil by metal oxide nanoparticles after water flooding at 26°C, 40°C, 50°C, 60°C. As an overview, it can be seen the properties of each nanoparticle. Al<sub>2</sub>O<sub>3</sub> aluminum oxide showed the highest oil recovery than other nanoparticles in that conditions. The reason for that is aluminum oxide greatly impacts the reduction of interfacial tension IFT rather than on wettability alteration. On other hand, SiO<sub>2</sub> silica oxide nanoparticles demonstrated the lowest oil recovery as the main characteristic for nanoparticles after water injection is the reduction of IFT. Thus, the quality of the work can be improved by comparing the results of oil recovery using nanoparticles as secondary and tertiary processes. In the case of using metal oxide nanoparticles as secondary recovery processes, the main mechanism for incremental oil recovery might be wettability alteration (Bayat E., September 2014).

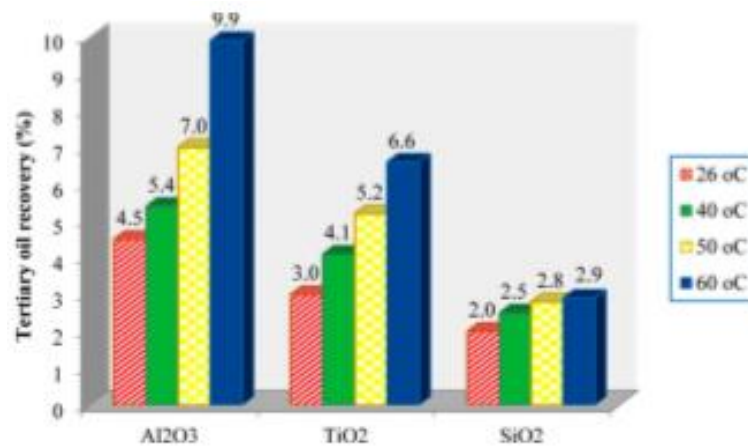


Figure 15. Recovery of oil by methal oxide nanoparticles after water flooding (Bayat E., September 2014)

Hu reported the results between TiO<sub>2</sub> titanium oxide nanoparticle in brine and water injection. The core flooding test was designed by the researcher. He compared recovery of oil at and after the breakthrough at Berea sandstone rock. The outcomes show that cumulative oil production was increased to 31.4% in comparison with waterflooding. However, recovery of oil was not raised at a higher than 20 ppm concentration of titanium oxide nanoparticle. This occurred due to the log-jamming mechanism as post breakthrough enhancement was observed at 500 ppm of titanium oxide nanofluid injection. Log-jamming is the type of pore channel plugging mechanism. It occurs when particles trap in a narrow zone after particles become untrapped with increasing pressure drop. The author also found that the wettability of Berea sandstone was changed towards strongly water-wet with increasing concentration of nanoparticles. Additionally, stabilizers inside nanofluid solution have to be accurately chosen, as permeability blockage was observed due to them (Hu Z., March 2016).

A nanofluid does not merge all the above-mentioned properties such as wettability alteration, IFT reduction, and lowering viscosity of oil for enhancing oil recovery. Since the mixture of nanofluids combine those characteristics, researchers conducted experiments to test this theory. Alomair and his colleagues experimented with single and mixed flooding of nanofluids to displace heavy oil in reservoir conditions, which is high salinity water and high temperature. It is shown in Figure 16 that the combination of silica and aluminum oxide nanofluid has demonstrated the highest recovery factor. Besides, they observed that using nanofluids as secondary recovery is more effective than using them as tertiary recovery process. For our case, we can do optimization on injection time (Alomair O.A., August 2015). It would be better to start before the breakthrough because it will help to reduce slug size as compared with starting from the beginning.

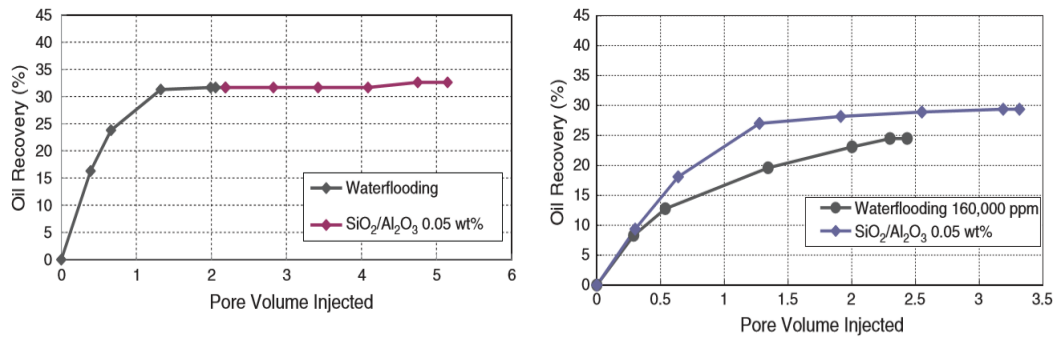


Figure 16. Recovery factors of waterflooding and mixture of nanofluids (Alomair O.A., August 2015)

Mohamed Tarek investigated the effects on the mixture of nanofluids of Al<sub>2</sub>O<sub>3</sub>, Fe<sub>2</sub>O<sub>3</sub>, and SiO<sub>2</sub> for oil recovery applications and different injection techniques. According to the information obtained combination of nanofluids have more advantageous than using them separately and the best possible concentrations of nanofluids are controlled by rock and fluid characteristics. In that case, the concentration of 35% Al<sub>2</sub>O<sub>3</sub>, 40% Fe<sub>2</sub>O<sub>3</sub>, and 25% SiO<sub>2</sub> was the most optimal as the main influence was Iron oxide. Furthermore, salinity does not impact the performance of nanofluids and nanofluid flooding is beneficial after water injection. Besides, he found that using a nanofluid slug rather than continuous injection would be cost-effective and nanoparticles with low salinity water show a minor rise in oil production following low salinity water flooding. He advises performing nanofluid injection at the earliest moment (Tarek, September 2015) Nevertheless, they did not show results of bump rate and permeabilities were different for each tested core.

However, the main challenge for nanofluids is the stability of nanoparticles in base fluids. The stability of nanofluid is measured by the zeta potential parameter. Zeta potential

shows the negative charge within the solution. Thus, if the zeta potential is zero, a nanofluid will be unstable. It means nanoparticles formed micro flock and then macro flock so that they ultimately settled out from base fluids. This might happen due to several factors such as the addition of positive ions, type of base fluids, and inaccurate dilution of nanoparticles. Three methods were proposed to avoid this problem. Firstly, the pH parameter has to be altered. It should differ from isoelectric point or IEP. Isoelectric point is the point where pH is not positive or not negative and zeta potential equals zero. Therefore, nanoparticle is unstable at IEP. According to Wen and Ding works on heat transfer of nanofluids, they suggested using pH value 7 to have stable nanofluids (Ding, March 2005). Secondly, surfactant can be added to make nanoparticles stable in a base fluid. However, the addition of surfactant will change the properties of nanofluids. Therefore, this method is rarely used in practice. And finally, the widely applied method for making stable nanofluid is ultrasonication. For this process, different ultrasonic tools are used but the main working principle of them is sending high-frequency waves to homogenize fluid. Ruan and Jacobi investigated the impact of sonication on the characteristics of nanofluids. It indicates that the quality of the thermal conductivity and rheology of nanofluids became better with increasing sonication time. However, increasing sonication time above 40 minutes, the properties of nanofluids turned to be worse. Therefore, the time of ultrasonication has to be accurately set, otherwise it will inversely affect on stability of nanofluid (Jacobi, February 2014).

## **2.4 Experimental studies of nano-assisted polymer flooding**

Cheraghian conducted experiments to compare results of heavy oil recovery factor at low salinity water and sandstone rock between TiO<sub>2</sub> titanium dioxide nanoparticle with partially hydrolyzed polyacrylamide (HPAM) polymer with separately used polymer flooding. They found that recovery is increased to 4% with nano-assisted polymer than individually used polymer in sandstone rock. The reason for that is titanium oxide nanoparticles changed the rheological properties of the polymer, particularly increased polymer's viscosity at low shear rates. However, such improvement of oil recovery depends on the concentration of nanoparticles, which have to exceed a certain amount of value ( $\geq 2.3$  wt%) and have to be less than 2.5 wt%. Additionally, the most optimal concentration of polymer was 3150 ppm, more than that resulted in unchanged oil recovery. He suggests for further work to perform the same experiment with other types of nanoparticles (Cheraghian, 25 May 2016).

Tushar Sharma and Stefan Iglauer studied the influence of nanofluids on polymers at low salinity water and sandstone rock for enhancing oil recovery. In particular, varying concentrations of silicon oxide nanofluids with polyacrylamide and with surfactant polymers are compared. Results show that the mixture of silica nanofluid with polymers or with surfactant polymers is less sensitive at high temperatures than surfactant polymer or individual polymers. The rock wettability changed to strongly water-wet and interfacial tension reduced with the addition of silicon oxide nanoparticles to polymers and surfactant polymers. This is the first experiment where nanoparticles were used with surfactant polymer for increasing oil production purposes (Tushar Sharma, November 2016).

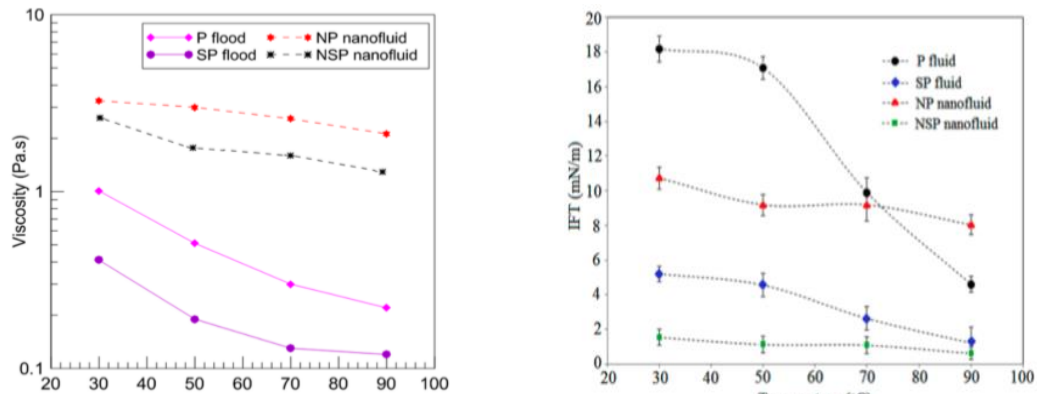


Figure 17. Impact of temperature on viscosity and on IFT of different solutions (Tushar Sharma, November 2016)

Figure 17 represents four core flooding experiments. Overall, the viscosity of nanofluid and polymer solutions are more stable than polymer or surfactant polymer in high temperatures, while polymer and surfactant polymers are not. Nano-assisted polymers better control mobility ratio among four mentioned fluids because it has the highest viscosity. Interestingly, the addition of surfactant to nanofluid polymers decreases viscosity, which might be due to the relaxation of the polymer. Thus, silica nanofluid (SiO<sub>2</sub>) shows the capability to increase the efficiency of chemical EOR.

Maghzi with colleagues studied the efficiency of SiO<sub>2</sub> silica nano-assisted partially hydrolyzed polyacrylamide polymer flooding at high salinity, heavy oil conditions. An injection test was performed by micromodel as well as salt concentrations were varied from 1400 ppm to 84000 ppm. Obtained results indicate that cumulative oil production slightly decreased with the addition of nanoparticles at high salinity, whereas the recovery factor of oil was drastically



reduced with using pure polymers at high salinity. In other words, the recovery factor of polymer and nanoparticle solution was greater than pure polymer flooding because nanoparticles resist polymer degradation with increasing salinity. This is known as ion-dipole interaction. The significance of the article is it gives a piece of valuable information about nanofluid-aided polymer flooding at high salinity conditions (Maghzi A., February 2014).

Laura Corredor, Brij Maini, and Maen Husein measured the stability and areal sweep efficiency of different types of silicon oxide nanoparticles and polymers. They tested HPAM and xanthan gum polymers. The results showed that silica nanoparticles are more stable when they are added to polymers than in distilled water and they didn't change shear-thinning to thickening behavior of polymers as well. The highest stability shows silica nanoparticles with HPAM solution. The areal sweep efficiencies are poor for all solutions except 1.0 and 2.0 wt% of silica nanoparticles with XG biopolymer after 1 PV injection shows favorable cases ( $M < 1$ ). The reason is silica nanoparticles improve the elastic characteristics of xanthan gum as its molecular structure is similar to gels. On the other hand, the addition of silicon oxide nanoparticles reduces the elastic properties of HPAM, which leads to an uncontrolled flooding process. This is the first published which investigated the impact of silicon oxide nanoparticle to xanthan gum biopolymer and the first experiment that conducted measurements of areal sweep efficiency of nanoparticle polymer solution in Hele-Shaw cell (Laura Corredor, October 2018).

Druetta and Pichhioni completed the reservoir simulation model in 2 dimensions with polymer and nanoparticles injection. Researchers considered complex processes such as reservoir heterogeneity, polymer and nanoparticle degradation, and adsorption on rock surfaces during the dynamic process. The results demonstrate that the first injection of nanofluid

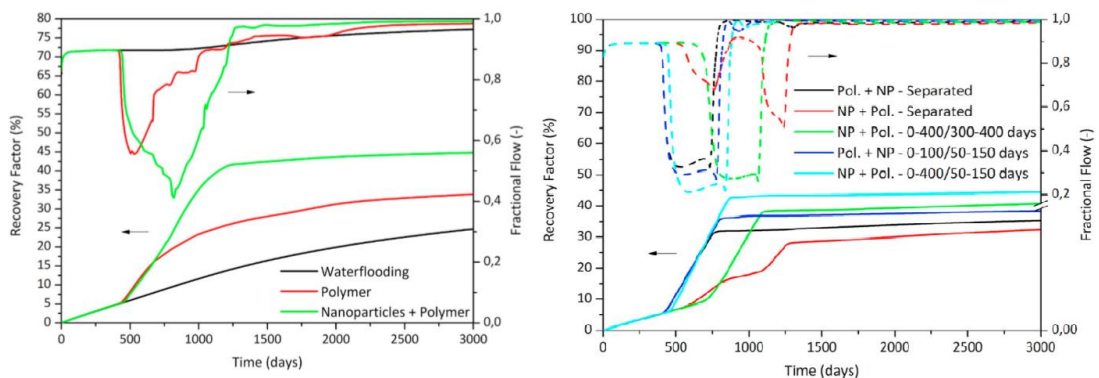


Figure 18. Recovery of factor and fractional flow versus time for different cases (Druetta P., 2019, February)

decreased polymer adsorption, consequently enhanced oil recovery. The authors suggest injecting first in order slug of nanoparticles, which alter wettability towards water-wet, as well as make it soak for a while in the reservoir. After that, polymer flooding will be a highly effective method to obtain more production. Besides, the recovery factor of nano-assisted polymer injection was increased up to 20.11% compare with waterflooding. The results of sensitivity analysis showed that injection time is an essential parameter that significantly impacts recovery efficiency. It should be extended as much as possible. The significance of the work is it gives useful injection strategies which can be applied in the field. However, the numerical model have to be confirmed with laboratory test and the rheology of nanofluid aided polymers require in-depth analysis (Druetta P., 2019, February).

Figure 18 shows the recovery factor of oil as a function of time. It can be seen from both line graphs that nano-assisted polymer is substantially efficient than other injection methods. Regarding the injection strategy, initially flooding the reservoir with nanoparticles shows satisfactory results rather than flooding simultaneously polymer and nanoparticles. Noticeably, the injection time of chemicals contributes significantly to oil recovery. It should be chosen accurately (Druetta P., 2019, February).

Yadav with colleagues investigated the impact of silicon oxide SiO<sub>2</sub> nanoparticles on the rheology of partially hydrolyzed polyacrylamide HPAM. The viscosity of the solution was measured with increasing shear rate at a high temperature of 90 °C. Obtained results indicate that the viscosity of the solution was linearly increased and showed viscoelastic properties at high temperatures with adding more concentrations of nanoparticles. Furthermore, the salinity negatively influences on rheology of polymer and nanoparticle solution, as there is more chance of “coiling”. However, the effect of salinity is lesser in nano-assisted polymer fluid than pure

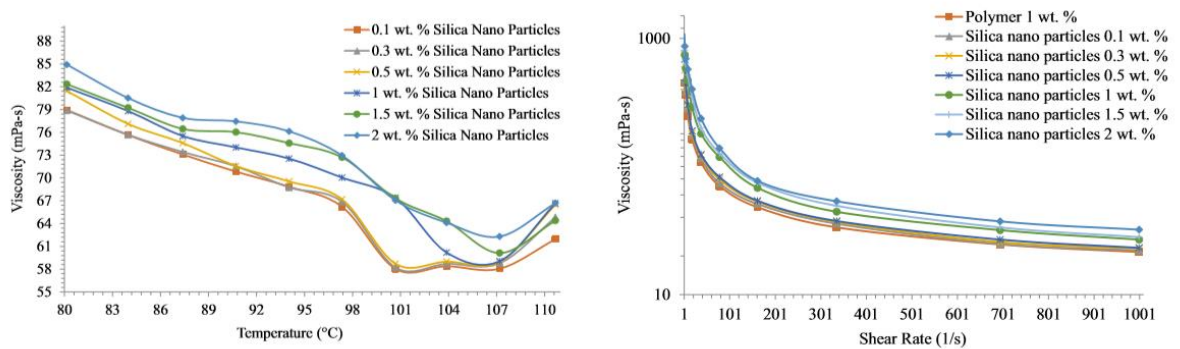


Figure 19. Rheological behaviour of polymer solution at different concentration of nanoparticles (Yadav U.S., 31 July 2019)

polymer. Thus, nanoparticles can be useful agents at high temperatures and high salinity during polymer flooding. The article is valuable because it shows the basic rheological properties of nanofluid aided polymer solution. Nonetheless, long-term and mechanical stability tests should be conducted to fulfill the work (Yadav U.S., 31 July 2019).

Figure 19 represents the rheological behavior of nanoparticle and polymer solution. As an overview, the viscosity of polymer solution increases with adding more concentration of silica nanoparticle. At high temperatures, partially hydrolyzed polyacrylamide HPAM and silicon oxide SiO<sub>2</sub> nanoparticles solutions shows viscoelastic behavior. Therefore, as aforementioned nanoparticles can be useful agents at high temperatures and high salinity during polymer flooding. However, the viscoelastic behavior of the solution has to be verified at a dynamic process such as the core flooding test (Yadav U.S., 31 July 2019).

Saha, Uppaluri, and Tiwari researched 5000 ppm xanthan gum polymer performance with silicon oxide SiO<sub>2</sub> nanoparticle for a heavy oil sandstone Berea core sample at 30°C, 80°C. The study area focused on the bulk properties of solution and core flooding experiment. The rheological behavior of solution was analyzed by rheometer, whereas IFT between heavy oil and solution was determined by surface tensiometer and Wilhelmy plate method. Emulsification was measured by an orbital shaker, while wettability alteration was identified by a drop shape analyzer. Researchers came up with results that show an increase of cumulative oil production for 18% at 80°C due to such as changes of wettability, IFT reduction, alteration in rheological properties, and emulsification stability between fluids. Additionally, they found that silica nanoparticle is stable in polymer solution, while nanoparticle is unstable in formation water. Therefore, nanoparticles can be used with polymer flooding rather than with water flooding processes. Regarding to bulk characteristics of nano-assisted polymer solution, the viscosity was increased even at high temperatures in comparison with pure polymer as well as the solution showed viscoelastic properties. IFT was reduced with increasing concentration of silica nanoparticles from 0.1wt% to 0.5wt%. However, IFT remained constant after 0.3wt% of silica nanoparticles. Thus, the authors suggested using 0.3wt% of SiO<sub>2</sub> nanoparticles and 5000 ppm of xanthan gum polymer as optimal concentrations. The wettability of the core sample was altered towards to strongly water with an increasing concentration of silica nanoparticles. The article offers useful material for further work processes, such as bulk properties of xanthan gum and silica nanoparticle solution their optimal concentrations, and results of the core flooding experiment. It covered all insights about silica nano-assisted xanthan gum polymer flooding at high-temperature conditions (Rahul Saha, 20 April 2018).

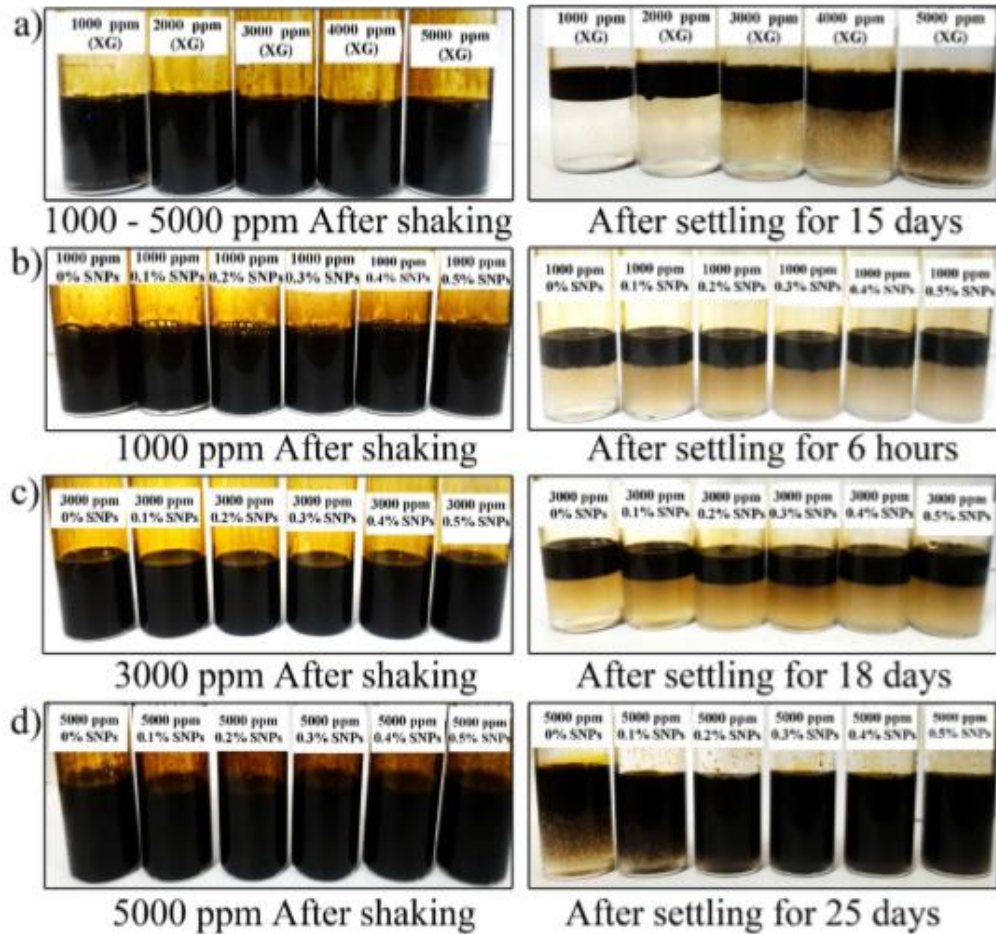


Figure 20. Emulsification between heavy oil and silica nanofluid aided xanthan gum polymer solution at different concentrations (*Rahul Saha, 20 April 2018*)

Figure 20 represents emulsification between heavy oil and silica nanofluid aided xanthan gum polymer solution at different concentrations. As an overview, 5000 ppm of xanthan gum and 0.3wt% of SiO<sub>2</sub> nanoparticles are optimal concentrations at 30°C. Below 5000 ppm of xanthan gum polymer as well as below 0.3wt% of silica nanoparticle concentrations are unfavorable for emulsification stability between fluids in the long term. Noticeably, above 0.3wt% of silica nanoparticles indicates emulsification stability. Thus, it will be cost-effective to choose lower concentrations of chemicals as possible but they have to be stable with each other in the long term.

Karl, Jagar, and Kamal completed an experiment about the influence of a mix of zinc oxide and silica oxide nanoparticles on recovery efficiency of low salinity biopolymer flooding. Experiments completed on carbonate core rock and xanthan gum were chosen as biopolymer. Nanoparticles were dispersed in low-salinity water and preserved for the long term to make it stable. IFT was determined by the pendant drop method at 30°C, 50°C, 70°C. Researchers

compared the results of IFT and recovery factors between nano-assisted polymer and water injections during core flooding experiments. It shows the reduction of IFT from 32 to 2 mN/m as well as increasing cumulative oil production to one and half times. Additionally, nano-assisted polymer injection shifted the relative permeability curve to the right due to a change of wettability. Generally, the article is useful because it focused on the reduction of IFT during low-salinity nanofluid-aided polymer flooding at carbonate rock. On the other hand, the work could be improved by direct measurements of wettability alteration. Thus, the reason for increasing cumulative oil production could be analyzed more deeply (Karl, January 2019).

### **3. Methodology**

The methodology was designed in accordance with the main objectives of the thesis. In this research, the combination of modified synthetic polymer and silica nanoparticles involves complex laboratory investigations to guarantee improvement in the recovery mechanisms. The primary target was to examine the stability of a combination of silica nanofluids and modified synthetic polymers in different salinities. Especially, the stability of silica nanoparticles was carefully studied through the use of zeta potential results as it was one of the main challenges to prepare a stable nanofluid. The secondary purpose was to screen optimum concentrations of silica nanoparticle and modified synthetic polymer that can tolerate high salinity, high-temperature conditions. Since silica nanoparticles demonstrated wettability alteration property, screening the optimum concentration for silica nanoparticles was done via contact angle measurements. Subsequently, the negative effect of combination between two chemicals, salinity, and temperature on properties such as stability was studied as well. Additionally, the combination of silica nanofluids and modified synthetic polymer, known as nano-assisted polymer solution, were tested with several screening variables in particular nanoparticle presence, temperature, salinity, the concentration of polymer, and thermal degradation. The results from these rheological experiments, zeta potential tests, and contact angle measurements would be integrated to identify the most appropriate nano-assisted polymer fluid for advanced research. The next stages were put forward to achieve the thesis goals and to guarantee the performance of nano-assisted polymer flooding for enhance oil recovery:

- The stability of combination of silica nanofluids and modified synthetic polymers in different salinities were assessed via zeta sizer;
- The optimum concentration of silica nanoparticle was selected on the basis of zeta potential and contact angle measurements;

- The optimum concentration of modified synthetic polymer was screened based upon comprehensive rheological tests;
- The effect of screened polymer concentration on the stability of silica nanoparticle was evaluated with zeta potential measurements;
- The target viscosity 4-5 cP was acquired with the nano-assisted polymer solution;
- The static adsorption of the combination of silica nanofluids and modified synthetic polymers were analyzed;

Sections materials and procedures present further details.

### 3.1 Materials

This part presents details of the materials that were utilized in laboratory work. Formation water, polymer, nanofluid, and carbonate core sample were used as materials.

#### 3.1.1 Carbonate core

Indiana limestone carbonate outcrop was used for the experiments. The core sample is 1.5 inches in diameter and is 12 inches in length, which was cut to 10 pellets with a 0.75-inch diameter.

#### 3.1.2 Formation water

The formation water composition of the Tengiz field was used to prepare nanofluid, polymer solution, and nano-assisted polymer solution. Table 1 shows the ionic agents to prepare brine, while Table 2 displays composition of ions (cations and anions) for 40 000 ppm salinity brine. These formation water was used for further experiments.

Table 1. Ionizing compounds

Salts	Weight percent, %
NaCl	84.3
CaCl <sub>2</sub> *2H <sub>2</sub> O	10.71
MgCl <sub>2</sub> *6H <sub>2</sub> O	4.98

Table 2. Composition of ions for 40 000 ppm brine

Ions	Required amount, ppm
$Na^+$	13600
$Ca^{2+}$	1590
$Mg^{2+}$	245
$Cl^-$	15062
<b>Total</b>	<b>40000</b>

### 3.1.3 Polymer

SAV 10 modified synthetic polyacrylamide polymer was used for this study. The polymer is in HPAM-based polymer group, where the commercial name is SUPERPUSHER SAV 10. The choice of this polymer was based on their properties to withstand harsh conditions due to a chemical structure ( (Jouenne, 2020), (Muhammad Rehan Hashmet, April 2017), (Song, et al., September 24 2020)). Harsh conditions refer to temperature up 120°C and water salinity of 185000 ppm. Polymers were supplied as a powder. They were purchased from SNF Floerger. The chemical structure of HPAM-based polymer group is illustrated in Figure 21.

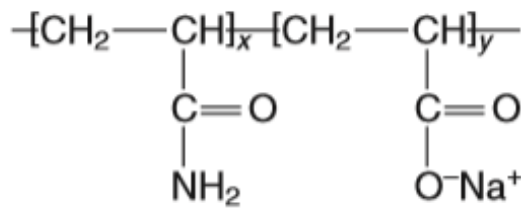


Figure 21. The chemical structure of HPAM-based polymer (Sheng, 2011)

### 3.1.4 Nanofluid

$SiO_2$  silicon oxide nanoparticle of was used in the experiment. Nanoparticle was purchased from SkySpring Nanomaterials, Inc. The nanoparticle was selected due to several properties ( (Abbas Roustaei, 17 August 2014), (Maghzi A., February 2014), (Ogolo N.A., April 2012)). One of the main characteristics is wettability alteration towards water-wet. Table 3 illustrates the following features of nanoparticles.

Table 3. The characteristics of nanoparticle

Type of nanoparticles	Size	Specific surface area (SSA)	Morphology	Density	Purity
Silicon oxide (SiO <sub>2</sub> )	10-20 nm	640 m <sup>2</sup> /g	Spherical	2.4 g/cm <sup>3</sup>	99.50%

## 3.2 Procedure

This segment shows parts of the project and their working processes, including wettability alteration, stability tests, rheology of fluids, long-term stability and static adsorption analysis.

### 3.2.1 Fluid preparation

Brine, polymer, nanofluids, and nano-assisted polymer solutions were prepared from a distilled water. The formation water was prepared by adding necessary quantity of salts namely  $NaCl$ ,  $CaCl_2 * 2H_2O$ ,  $MgCl_2 * 6H_2O$ . The required amount salts were mentioned in materials sections Table 2.

The brine salts were added after the preparation of the polymer solution. Dry polymer was added uniformly to distilled water with a magnetically driven stirrer to prevent the formation of “fish eyes” at 600 rpm. After all, polymers were added, a magnetic stirrer was set to a low rate (~150 rpm). This is used to avoid mechanical degradation of the solution. Then, the polymer solution proceeded at a low rate for 3 hours. Brine salts were added to polymer fluid at a low rate for 1 hour and kept the solution overnight. The polymer solutions were prepared in several salinities (0, 2400, 4800, 9800, 19800, 26600, 40000, 80000, 183000 ppm).

Nanofluids were prepared with reference to the methodology of the literature review. Nanoparticles were added to distilled water and then were placed to ultrasonic homogenizer at 70°C for 45 minutes. Figure 22 shows ultrasonic homogenizer that was used in the study. After the fluid was cooled, the brine salt was added at a low rate for 1 hour.

Nano-assisted polymer fluids were used in the work. They were prepared with reference to the methodology of the literature review. Nanoparticle was added to distilled water and then was placed to ultrasonic homogenizer at 70°C for 45 minutes. Figure 22 shows ultrasonic homogenizer that was used in the study. After the fluid was cooled, dry polymer was added uniformly to the already prepared solution with a magnetically driven stirrer to prevent the formation of “fish eyes” at 600 rpm. After all polymers were added, a magnetic stirrer was set to a low rate (~150 rpm). This is used to avoid mechanical degradation of the solution. Then, nano-assisted polymer fluid proceeded at a low rate for 3 hours. After, brine salts were added to nano-assisted polymer fluid at a low rate for 1 hour and kept the solution for the night.



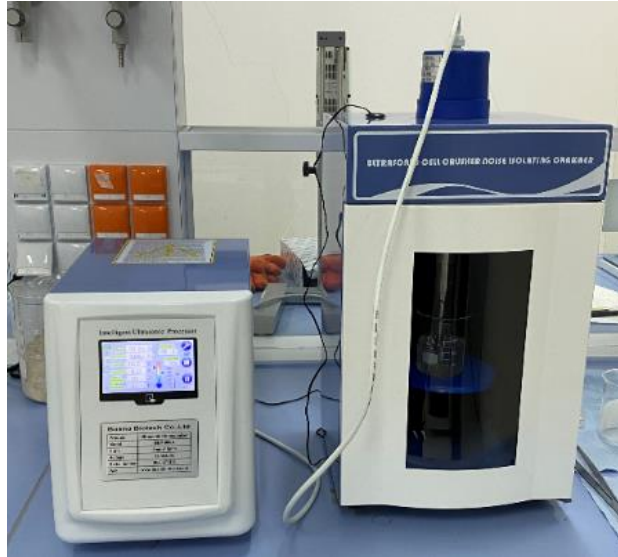


Figure 22. Ultrasonic Homogenizer

### 3.2.2 Contact angle measurements

The contact angle measurements were completed to screen the optimum concentration of silica nanoparticles. Primarily, carbonate pellets were dried in the oven then were aged in brine for one week. Then, the cores were aged in a light oil for 100 days at 120°C to achieve the oil-wet condition. Secondary, the captive bubble method was used to estimate wettability of core via OCA 15EC as shown in Figure 23, where an ambient phase was formation water, a dropping phase was a light oil from Aktobe. The captive bubble method is the most relative approach to reproduce the original reservoir environment as oil drops from bottom to up. The contact angles were measured of oil-wet carbonate pellets. Subsequently, the cores were stored in silica-based nanofluids for 48 hours. Afterward, the contact angles were measured to examine the effect of nanofluids on wettability alteration. The measurements were completed three times for one test to obtain representative results.

Additionally, the wetting angle was measured between the dropping phase (a light oil) and carbonate surface. Thus, the oil spreading over the carbonate rock surface was distinguished as wetting phase. The wettability state was evaluated by the following range :

- Oil wet,  $0^\circ < \theta < 75^\circ$
- Neutrally wet,  $75^\circ < \theta < 105^\circ$
- Water wet,  $105^\circ < \theta < 180^\circ$

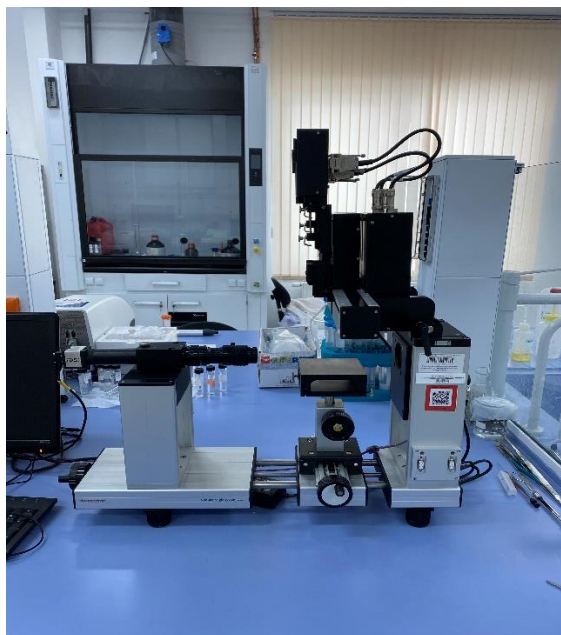


Figure 23. OCA 15EC

### 3.2.3 Zeta potential tests

Zeta potential tests were performed to examine the stability of silicon oxide nanofluids and nano-assisted polymer solutions at various concentrations of chemicals and salinities. In the first instance, nano-assisted polymer fluids were prepared with varying concentration of SAV 10 polymer (0, 500, 1000, 1500, 2000, 3000 ppm) and silica nanoparticles (0.05, 0.1, 0.15 wt%) at different salinities (0, 2400, 4800, 9800, 19800, 26600, 40000, 80000, 187000 ppm). The solutions were prepared according to API standards. Later, after fluids preparation, their stabilities were measured using Zetasizer Nano ZS electric potential measurement tool, as shown in Figure 24. Following the procedure, each test was measured three times to acquire high-quality measurements. Overall, the zeta potential tests were conducted to select the optimum concentration of silica nanoparticles as well as to screen the optimum salinity. The screening of optimum concentration was based on maximum stability values among all measured samples. The criteria of selection of the optimum salinity relied on the results, where silica nanofluid showed stability in the highest salinity. Above the highest salinity, silica nanofluid showed unstable values.



Figure 24. Zetasizer Nano ZS

### 3.2.4 Rheology experiments

The prepared polymer and nano-assisted polymer fluids were tested to investigate the effect of nanoparticle presence, temperature, salinity, and concentration of chemicals on the rheological behavior of fluid. It was completed by Anton Paar MCR 301 rheology measuring device, as shown in Figure 25. A cylindrical measurement system was used as it can operate at high temperatures. The experiments were performed from room temperature up to 80°C with different salinities (0, 2400, 4800, 9800, 19800, 26600, 40000 ppm) and with varying concentration of SAV 10 polymer (500, 1000, 1500, 2000, 3000 ppm) and silica nanoparticles (0.05, 0.1, 0.15 wt%). Consequently, the rheological experiments were fulfilled to mainly screen the best possible concentration of SAV 10 polymer. The optimum concentration was selected by meeting the target viscosity of 4-5 cP at  $10\text{ s}^{-1}$  shear rate, 80°C. Additionally, the selected concentration of polymer had to show the maximum viscosity among measured sample at high salinity, high temperature conditions. In accordance with these standard, the best possible concentration of SAV 10 polymer was elected for the prospective combination with  $\text{SiO}_2$  nanoparticle.



Figure 25. Anton Paar MCR 301

The best nano-assisted polymer solution was selected based on the following criteria:

- The optimum salinity was selected where silica nanofluid showed stability in the highest salinity. Above the highest salinity, silica nanofluid showed unstable values;
- The optimum concentration of silica nanoparticle was screened according to maximum stability values among all measured samples;
- The optimum concentration of SAV 10 polymer was selected by meeting the target viscosity of 4-5 cP at  $10 \text{ s}^{-1}$  shear rate,  $80^\circ\text{C}$ .

The remaining two experiments, long-term stability test, and static adsorption analysis have been done on the screened concentrations of nano-assisted polymer solution.

Figure 26 illustrates the flow chart of the experiments. It shows the way of selecting the most effective nano-assisted polymer solution. The sequence of the tests is becoming clear at the moment.

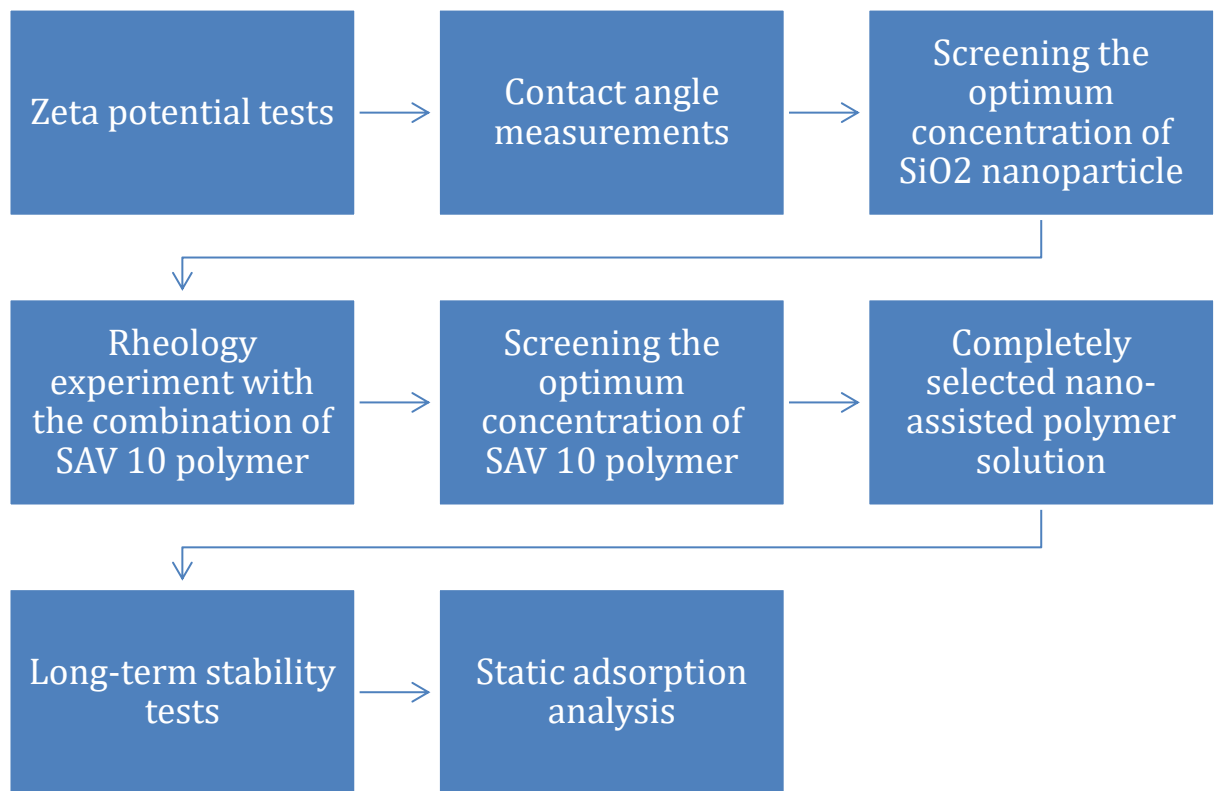


Figure 26. The flow chart of the experiments

### 3.2.5 Long-term stability tests

The long-term stability tests were performed with a selected concentration of nano-assisted polymer solution. The experiment was conducted to examine the effect of high temperature (80°C) on nano-assisted polymer fluid over a long period of time. It was achieved via Anton Paar MCR 301 and Zetasizer Nano ZS. Anton Paar MCR 301, particularly parallel plate measurement system was used to measure the rheology of solutions, while Zetasizer Nano ZS was utilized to determine stability of nanosuspension in polymer fluids. Thus, combination of  $SiO_2$  nanoparticle and SAV 10 polymer was prepared at selected salinity. Then, the fluid samples were stored at 80°C in an oven, after they were tested daily basis at room temperature.

### 3.2.6 Static adsorption analysis

Static adsorption analysis was completed using UV Spectrophotometer equipment. Primarily, 5 fluid samples (4 nano-assisted polymer fluids and 1 nano-assisted polymer solution with a carbonate core) and 1 baseline solution (formation water) were prepared in the laboratory, then were measured by UV Spectrophotometer. 5 fluid samples had a screened concentration of SAV 10 polymer and varying concentration of silica nanoparticles 0.025, 0.05, 0.075, 0.1 wt%.

Secondly, crashed carbonate core outcrops were added to fluid samples in the ratio of 1:3, afterward, solutions were stored 1 day in a roller. After, the samples were taken from solutions and were tested again in UV Spectrophotometer to determine the adsorption of fluids, as shown in Figure 29. Then, the calibration curve was generated from absorption measurements to obtain adsorption results. The data's from the calibration curve were chosen from the highest absorption values at a certain wavelength, where the y-axis is absorbance and x-axis  $SiO_2$  nanoparticle concentration. It was extrapolated to determine silica nanoparticle concentration at any absorbance, as illustrated in Figure 27.

$$y = kx + b, \rightarrow \text{Absorbance} = k * \text{NPs concentration} + b$$

$$\text{Absorbance} - b = \text{Corrected ABS} = k * \text{NPs concentration}$$

Figure 27. The relationship between absorbance and silica nanoparticle concentration

The silica nanoparticle concentration after the addition of carbonate core samples was calculated with the help of the above linear equation, where absorbance was generated from a UV Spectrophotometer. Finally, the adsorption was estimated by knowing the concentration of both solutions, as indicated in Figure 28.

$$\text{Adsorption} = \left[ 1 - \left( \frac{\text{NPs concentration after addition of rock}}{\text{NPs concentration}} \right) \right] * 100\%$$

Figure 28. Adsorption calculation

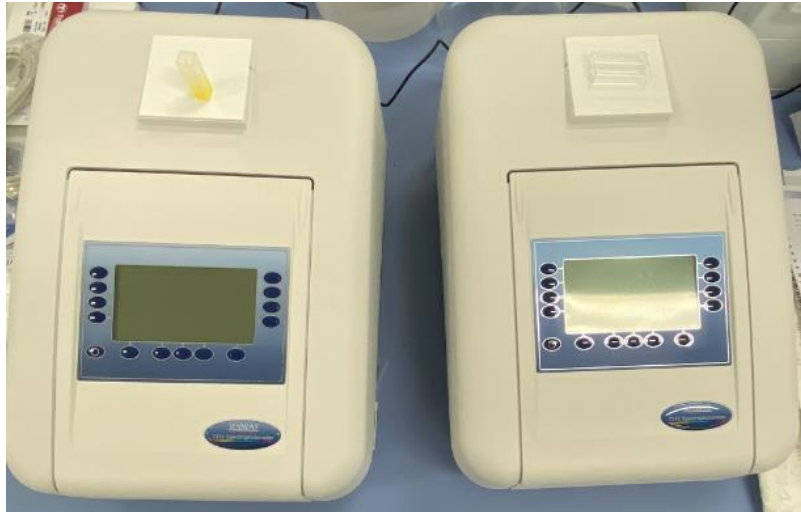


Figure 29. UV Spectrophotometer

## 4. Results

Different tests were conducted to achieve the best nano-assisted polymer fluid for harsh conditions to be utilized for EOR in carbonate rocks. It started by determining the optimum concentration of nanoparticles. Since silica nanoparticles can change wettability, the screening of concentration was based on the analysis of change in the contact angle values. Then, the stability of silica nanofluid and nano-assisted polymer solutions were tested in accordance with zeta potential values. Thus, after contact angle and stability measurements, the most effective nanofluid was chosen for the next experiments. The results will be presented in sections referred to as contact angle measurements and zeta potential tests.

After selecting the most effective nanoparticle, the screening optimum concentration for modified synthetic polymer was completed by rheological tests. This was done with the combination of selected nanoparticles. The assessment of the stability of a combination of nanofluids and polymers in various conditions was conducted by quantifying zeta potential values via a zeta sizer. Additionally, the following experiments were designed to investigate the effect of nanoparticle presence, temperature, salinity, and concentration of chemicals on the rheological behavior of nano-assisted polymer fluids. Importantly, it allowed us to select the best concentration of polymer. This was completed according:

- The maximum viscosity from concentrations 500 to 2000 ppm;
- The maximum viscosity at varying salinity and temperature;
- Meeting the target viscosity at  $10\text{ s}^{-1}$ ,  $80\text{ }^{\circ}\text{C}$ ;

Ultimately, the silica nanoparticle that demonstrated the highest wettability alteration towards water-wet and modified synthetic polymer that established the highest viscosity through varying concentration, salinity, and temperature were integrated to ensure improvement in recovery mechanisms. The screened nano-assisted polymer fluids were tested for long-term stability and adsorption. This was done to examine the effect of time, temperature on the viscosity of the selected solution, and adsorption rate of nanoparticles in polymer solutions. The results of long-term stability have to meet the target viscosity of 4-5 cP to provide a better mobility ratio. Regarding the static adsorption analysis, it will demonstrate the amount of nanoparticles that will adhere to the surface of carbonate rock. This would be useful information to consider the link between the wettability alteration and adsorption of the selected solution.

## 4.1 Contact angle measurements

Three concentrations of silica nanofluid were used for the study. The concentrations were 0.05, 0.1, and 0.15 wt% of silicon oxide nanoparticles at 40 000 ppm salinity. The effect of different solutions on the wettability alteration was compared with each other to identify the optimum concentration. The screening criteria for the determination of optimum concentration is based on the maximum alteration of oil/brine/carbonate rock contact angle towards the water-wet state.

Results indicate that overall silicon oxide nanofluids alter wettability. The maximum alteration of carbonate rock wettability towards water-wet occurred by silica-based nanofluid with 0.1 wt % concentration. On the other hand, 0.05 and 0.15 wt % silica nanofluid concentrations demonstrated roughly the same change of wettability. Thus, 0.1 wt % silicon oxide nanofluid was chosen for further experiments.

Figure 30 represents the relationship between contact angle difference and nanoparticle concentration. As above stated, the highest change in contact angle occurred by silica-based nanofluid with 0.1 wt % concentration. At the same time, 0.05 and 0.15 wt % silica nanofluid concentrations showed about similar change of wettability. It might be explained by the stability of the solutions. The stability of silica nanofluid with a concentration of 0.15 wt% possibly decreased while performing the experiment. Therefore, it was not significantly affected by the change of contact angle. Simultaneously, the impact of 0.05 wt% silica nanofluid on wettability alteration was not substantial because it was not enough amount of nanoparticle to change more contact angle.

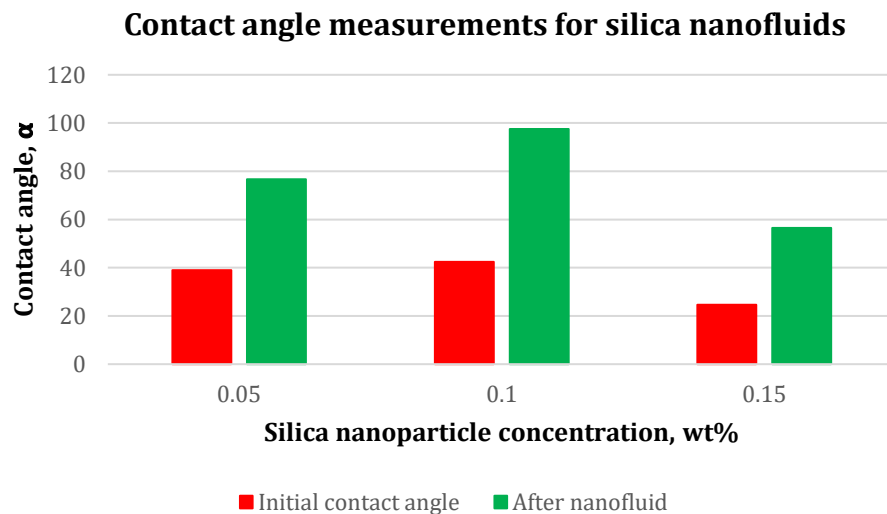


Figure 30. Contact angle vs. silica nanoparticle concentration



Table 4 illustrates the results of contact angle measurements. As an overview, the first column and second columns show the change in contact angle of carbonate core pellets with the function silica nanoparticle concentration.

Table 4. Results of contact angle measurements

Initial CA	After CA	Concentration of nano, wt%	The differen. CA
39	76.7	0.05	37.7
42.4	97.5	0.1	55.1
24.6	56.5	0.15	31.9

Figure 31 shows the visual influence of silicon oxide nanofluid on the wettability of a carbonate rock. The oil-aged carbonate pellets were used to measure contact angles. On the left side of Figure 31, it is seen that the pellets were oil-wet where a light oil from Aktobe spread to the surface of carbonate rock. The ambient phase was formation water, while the dropping phase was a light oil. Consequently, it demonstrates that silica oxide nanofluid has the property to alter the wettability of carbonate rock towards an intermediate water-wet state. However, wettability alteration depends on the concentration of injecting silicon oxide nanofluid. The maximum conversion in the wettability state occurred by 0.1 wt% silica nanofluid. Therefore, it was selected as the best nanofluid for further experiments that could significantly increase oil production from carbonate reservoirs. The results of 0.05 wt% and 0.15 wt%  $SiO_2$  nanofluid might be defined by the stability of solutions. As previously discussed, the stability of 0.15 wt%  $SiO_2$  nanofluid probably went down while conducting measurements. As a result, it was not substantially influenced by the alteration of the wettability state. At the same time, the effect of 0.05 wt%  $SiO_2$  nanofluid on the change of contact angle was not considered because it was not sufficient concentration of nanoparticle to maximize further contact angle.



Figure 31. Contact angle measurements of a) 0.05 wt%; b) 0.1 wt% and c) 0.15 wt%.

## 4.2 Zeta potential tests

NanoComposix, the laboratory specializing in nanoparticles, defined zeta potential analysis as “the method of establishing the surface charge of nanoparticles in solution.” Nanoparticles contain the surface charge which appeals oppositely charged ions. Nanoparticles proceed with this a double layer ion. It can be measured to determine the extent of a negative charge within the solution. The electric potential at the edge of the double layer is zeta potential, as shown in Figure 32 (NanoComposix, 2020).

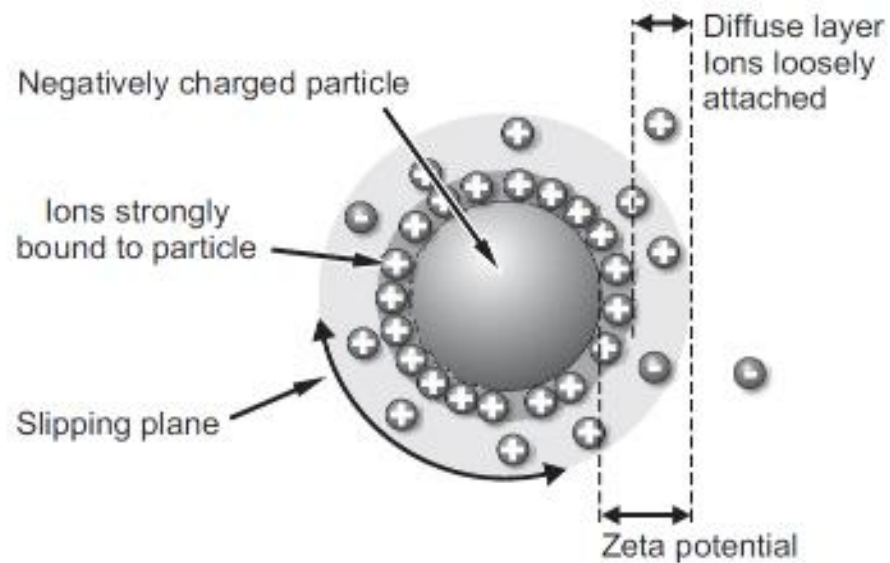


Figure 32. Illustration of zeta potential definition (NanoComposix, 2020)

One important use of zeta potential is that it can be used to forecast the stability of particles. Zeta potential of less than -60 mV or above 60 mV will have great stability. Conversely, zeta potentials in the range from -10 mV to 10 mV are in danger of rapid agglomeration. Therefore, the stability of fluids was identified based on this “rule of thumb”.

Firstly, the stability of nanofluids with 0.05 wt % concentration of silicon oxide nanoparticles were measured with different salinities (0, 2400, 4800, 9800, 19800, 26600, 40000, 80000, 183000 ppm). It was determined that silica nanofluids were unstable at 80000, 183000 ppm salinity. Consequently, further experiments proceeded with maximum salinity (40000 ppm), where silica nanofluid was more or less stable.

Table 5 illustrates the zeta potential values of 0.05 wt%  $\text{SiO}_2$  nanofluid in different salinities. As an overview, it can be seen that stability of the nanofluid decreases with increasing salinity. In other words, salinity significantly affects the zeta potential of silica nanofluid. This is explained by the relationship between the number of ions formation water and the electric double layer. The electric double layer is not contracted at low salinities because the amount of ions is low. It implies high zeta potentials values or stable nanofluid. On the other hand, the electric double layer is more compressed with increasing salinity as the number of ions are rising. Consequently, there is low zeta potential or unstable nanofluid. At particular salinity, the electric double layer will breakdown. It will turn to the same ambient exiting the nanoparticles vulnerable to agglomeration (*NanoComposix, 2020*).

Table 5. Zeta potential results of 0.05 wt% silica nanofluid with increasing salinity

Zeta potential, mV	Salinity, ppm
-34.8	1200
-31.35	2400
-29.2	4800
-25.19	9800
-20.7	19800
-16.37	26600
-5.28	40000
4.16	80000
10.7	183000

Then, zeta potential tests were completed with 0.05, 0.1, and 0.15 wt% of silica nanoparticles and 0, 500, 1000, 1500, 2000 ppm of polymer concentrations at 40 000 ppm salinity. Overall, nano-assisted polymer solution stability increases with increasing concentration of polymer. According to the result, 0.15 wt% silica-based nano-assisted polymer fluid is the least stable. On the other hand, similar results can be noticed with 0.05 and 0.1 wt% of silica-based nano-assisted polymer solutions. Probably, the optimum concentration for silica nanoparticles is 0.1 wt% at 40 000 ppm salinity, while the optimum concentration possibly for polymers is 2000 ppm at 40 000 ppm salinity.

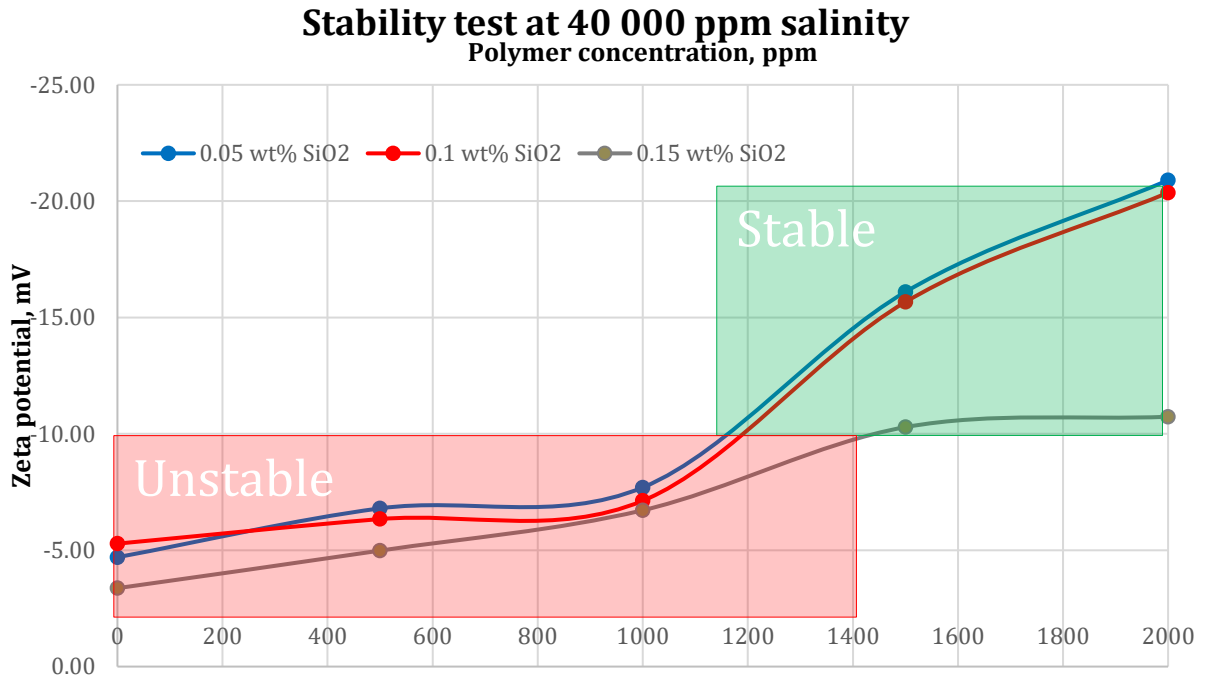


Figure 33. The relationship of stability nano-assisted polymer solutions with increasing polymer concentration

Figure 33 shows the dependence of nano-assisted polymer solutions on the concentration of polymer. It is clear that nanoparticles in the combined solution are becoming stable with the addition of modified synthetic polymer. SAV 10 polymer prevents agglomeration of silica nanoparticles due to lower suppressed electric double layer compared with pure silica nanofluid. This might be explained by the distribution of ions in brine between polymer solution and nanoparticle. Since positive and negative ions attract to each other, polymer structure will be “coiled” at high salinities, where polymer is a long-chained molecule that is negatively charged. In presence of high salinity brine, positive cations of brine ( $Na^{2+}$ ,  $Ca^{2+}$ ,  $Mg^{2+}$  and etc) will replace negatively charged anions of polymer. Thus, less amount of ions in brine will affect the electric double layer. It implies a more stable nanoparticle in the combined solution of silica nanoparticle and modified synthetic polymer fluid. The following experiments will reveal the stability of polymer in nano-assisted polymer solutions.

### 4.3 Rheology experiments

The study of the rheological behavior of the polymer separately is one of the main priorities for the effective application with nanoparticles as EOR method. Consequently, modified synthetic polymer was firstly tested to ensure stability at harsh conditions. In the research, SAV 10 modified synthetic polymer was utilized that belongs to HPAM-based group. The first parameter which impacts viscosity is the stability of the polymer. Polymer chains have to remain its structure inside formation. If for any reason, the long molecule structure of polymer breaks, so it will mean that polymer does not work. This might happen at high pressure, applied mechanical force, or high salinity. The idea of evaluating the stability of polymers is to measure viscosity at different temperatures or at different times. Thus, it is critical to consider the rheology of polymer. Polymer rheology is impacted by the molecular weight of polymer, polymer concentration, water salinity, shear-thinning behavior.

Figure 34 indicates SAV 10 polymer rheology with increasing concentration. Generally, it can be seen that modified synthetic polymer behaves as a non-Newtonian fluid with an increasing shear rate. It mainly shows shear thinning properties at a high shear rate except 500 ppm SAV 10. Additionally, the viscosity of the polymer becomes higher with increasing concentration. SAV 10 polymer with concentration 2000 ppm satisfy two criteria of screening the optimum concentration for the polymer which are:

- The maximum viscosity from concentrations 500 to 2000 ppm;
- Meeting the target of 4 cP viscosity at  $10\text{ s}^{-1}$ ,  $80\text{ }^{\circ}\text{C}$ ;

The following rheology experiments were proceeded with 2000 ppm SAV 10 to test for the remaining criteria of the selection of the most effective polymer with nanoparticles.

Figures 35 and 36 present 2000 ppm SAV 10 rheology with increasing temperature and salinity. In general, the viscosity of the solution reduces with increasing temperature and salinity. The stability of polymer becomes weaker with increasing salinity as there is more chance of “coiling”. Therefore, the most expedient salinity is 40000 ppm where the polymer meets the target viscosity of 4 cP.

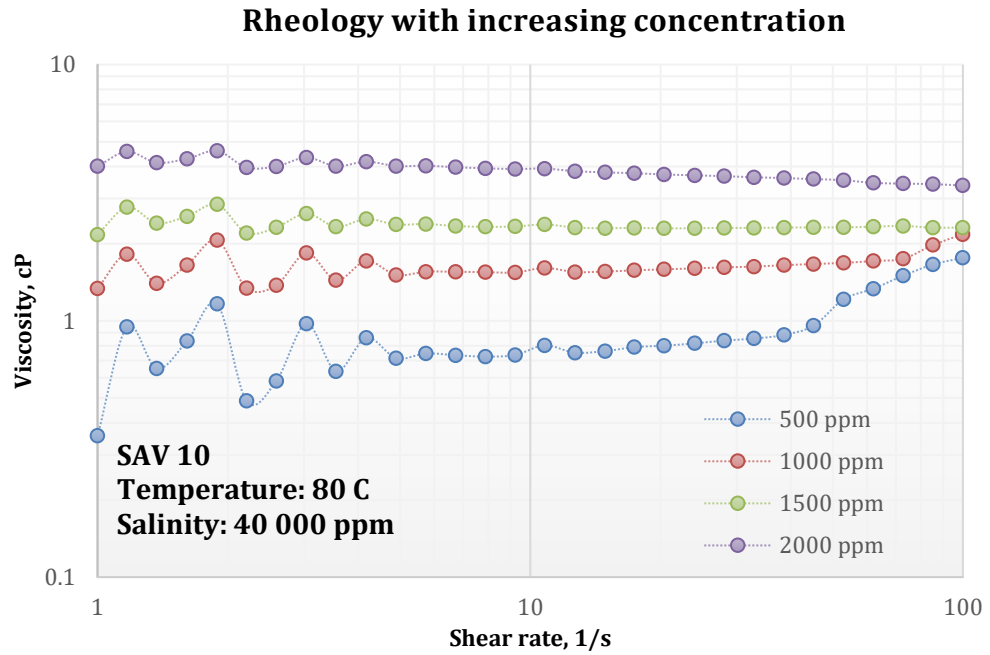


Figure 34. SAV 10 rheology with increasing concentration

The results display that SAV 10 modified synthetic polymer can withstand harsh conditions, as shown in Figures 35 and 36. The optimum concentration for the polymer is 2000 ppm because it meets the last criteria, where the first two requirements were satisfied by the mentioned test (Figure 34). The remaining essential was:

- The maximum viscosity at varying salinity and temperature.

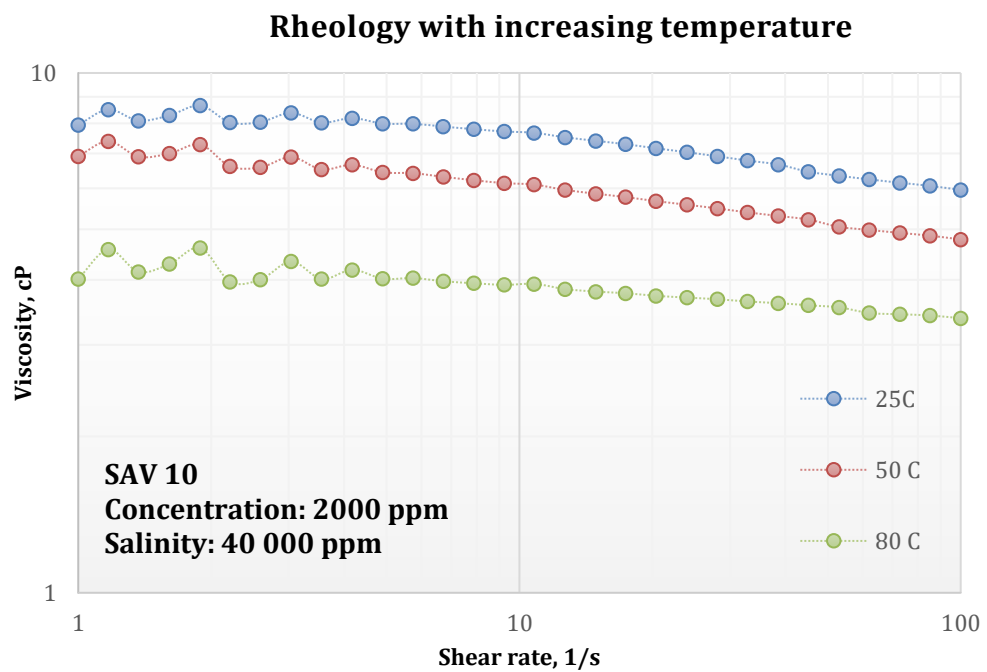


Figure 35. Rheology of SAV 10 with increasing temperature

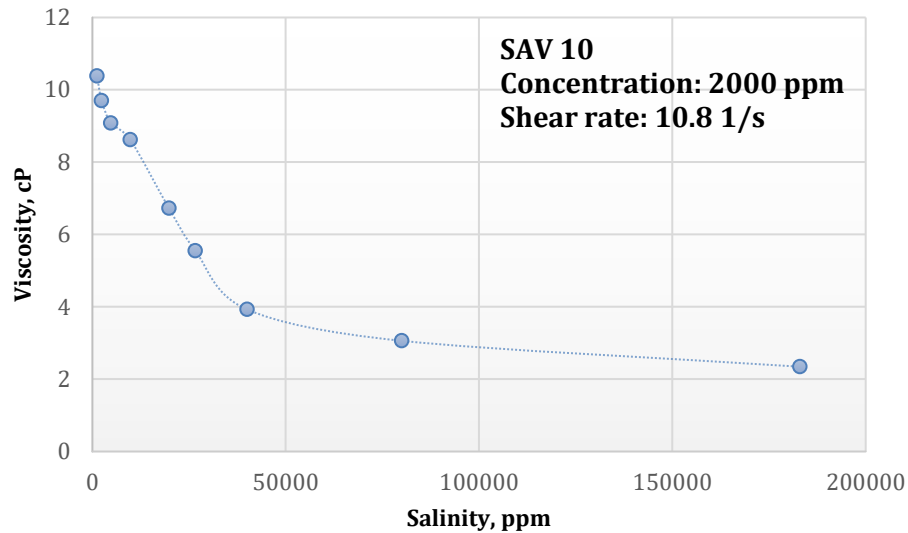


Figure 36. The reduction of SAV 10 viscosity with increasing salinity

Then, the prepared nano-assisted polymer fluids were tested to investigate the effect of nanoparticle presence, temperature, and concentration of chemicals on the rheological behavior of fluid.

The experiments were performed from room temperature up to 80°C with selected concentrations of SAV 10 polymer 2000 ppm and silica nanoparticles (0.05, 0.1, 0.15 wt%) at 40000 ppm salinity. Subsequently, the rheological experiments were fulfilled to mainly test the stability of polymer combination with nanoparticles.

Results display that increasing the concentration of polymer increases the viscosity of the solution while rising temperature decreases the viscosity as was expected (Figure 34 and 35). As an overview, the addition of nanoparticles makes the polymer fluid more viscous in all cases. Figure 37 indicate that polymer viscosity rising with increasing concentration of silica nanoparticle. Adding 0.1 wt% of silica nanoparticle can increase viscosity of SAV 10 polymer solution to 23.5 %, where the viscosity of nano-assisted polymer fluid become 4.85 cP at  $10 \text{ s}^{-1}$ , 80°C. It implies that the mobility ratio of the combination of nanoparticle and polymer is better than the mobility ratio of pure polymer solution. Figure 38 makes it clear that the addition of silica nanoparticles increases the viscosity of the SAV 10 modified synthetic polymer solution.



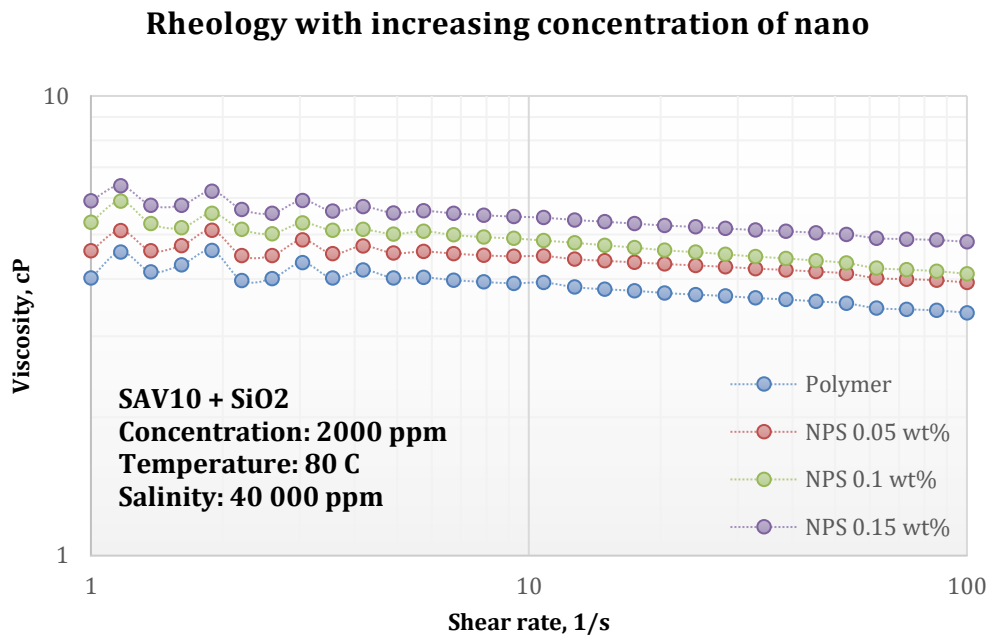


Figure 37. Rheology of nano-assisted polymer fluids with increasing concentration of silica nanoparticle

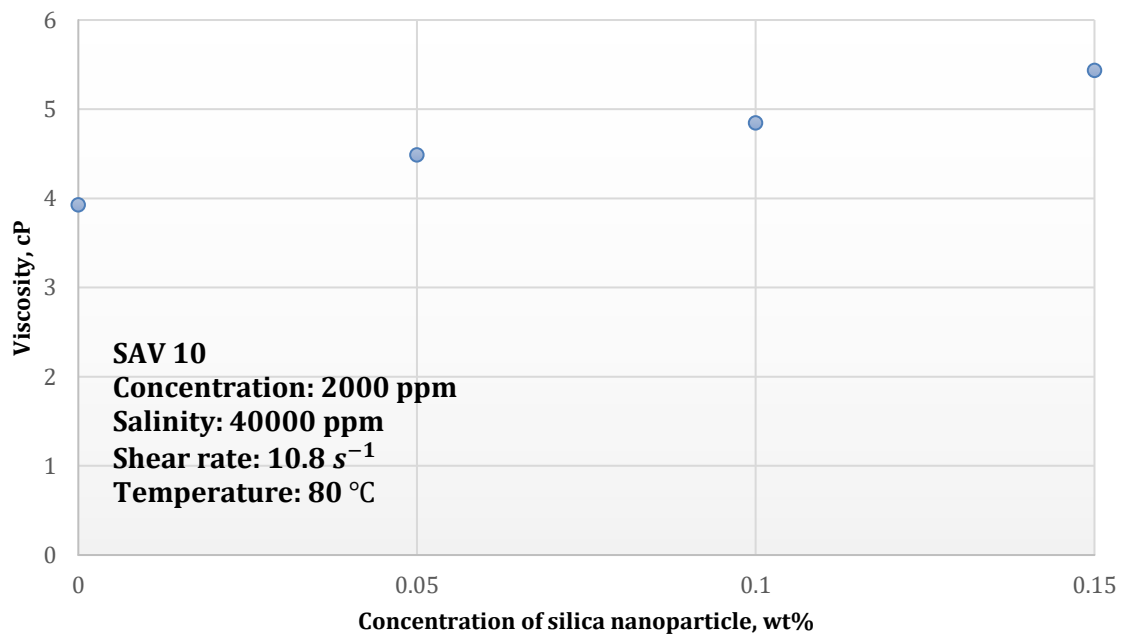


Figure 38. Effect of silica nanoparticle on viscosity of SAV 10 polymer solution

Figure 39 demonstrates the rheology of nano-assisted polymer solution with increasing concentration of SAV 10 polymer from 500 to 2000 ppm. We can state from the plot that 0.1 wt% silica nanofluid behaves as a Newtonian fluid, while it indicates non-Newtonian behavior with the addition of modified synthetic polymer with shear-thinning property. The highest viscosity among measured fluids is 0.1 wt% silica nano-assisted 2000 ppm polymer solution. 0.1 wt%  $SiO_2$  nanofluid, 2000 ppm SAV 10 polymer, and a combination of nanoparticle and polymer solutions were compared to visually illustrate the difference as shown in Figure 40. Nano-assisted polymer solution is the best choice than other solutions. Therefore, Figure 41 display the dependence of NPS to the temperature from 25°C to 80°C. A similar behavior between polymer and nano-assisted polymer solutions can be noticed, however NPS has more efficient rheology due to the presence of nanoparticles.

### Rheology of nano-assisted polymer solution

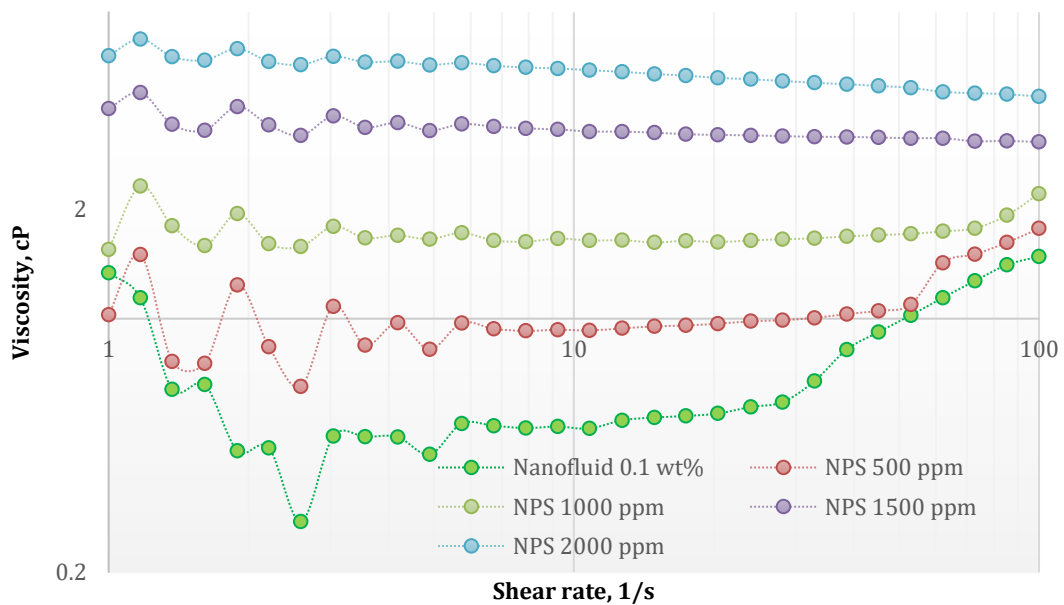


Figure 39. Rheology of nano-assisted polymer solutions with different concentration of polymer

## Comparison of solutions

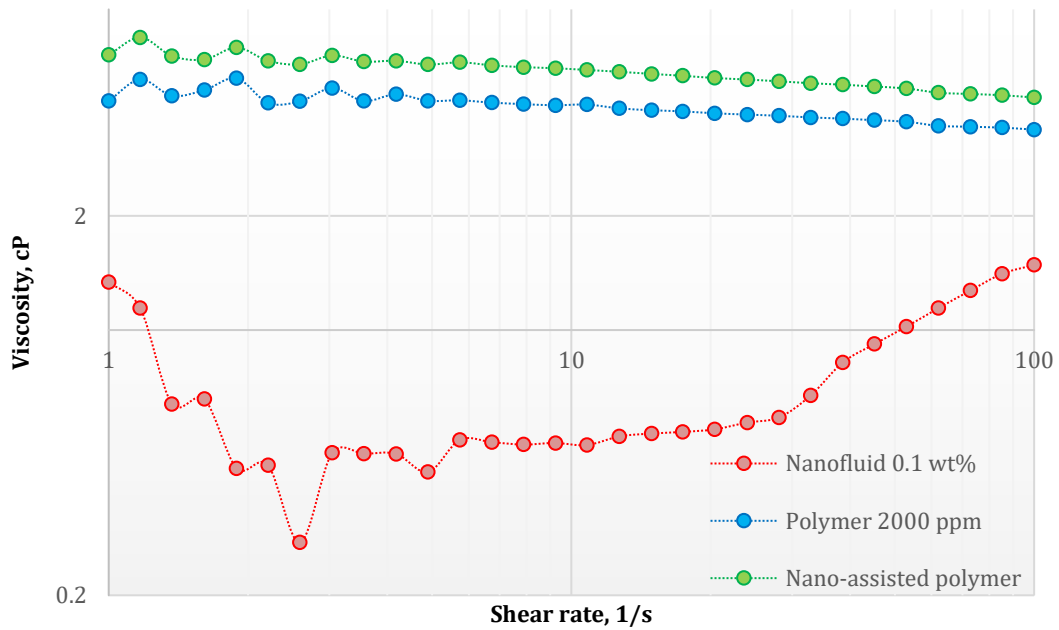


Figure 40. Comparison of solutions

## Rheology of nano-assisted polymer solution

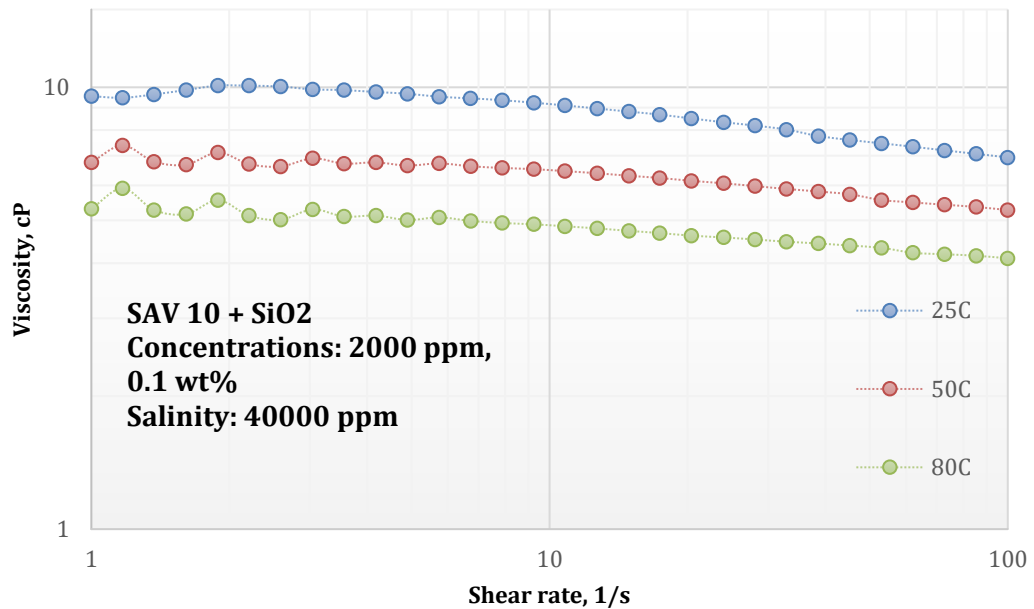


Figure 41. Rheology of 0.1 wt% silica nano-assisted 2000 ppm polymer solution with varying temperature

#### 4.4 Long-term stability tests

Nano-assisted polymer solution with 2000 ppm SAV 10 polymer, 0.1 wt % SiO<sub>2</sub> nanoparticles concentrations were selected for the long-term stability test. This was done to examine the stability of the solution for a long period at high temperatures. The nano-assisted polymer solution has to sustain stability through harsh conditions with time. The stability of synthetic polymer will reduce with increasing number of carboxyl. It occurs at high temperatures because the number of carboxyl groups rises with increasing hydrolysis (Sheng, 2011)F. On the other hand, nanofluid agglomerates with high temperature and time, as the electric double layer becomes more compressed. Therefore, the appropriate nano-assisted polymer solution have to keep half of its initial viscosity values during test interval. It implies that the long-term stability test required an experiment to validate the stability of a combination of nanoparticle and polymer solution.

Results demonstrate that nano-assisted polymer fluid was stable for a month at 80°C. The viscosity of the solution rapidly decreased for the first week as shown in Figure 42. Then, it remained consistent for the rest of the time. Figure 43 demonstrates that the appropriate nano-assisted polymer solution kept 50% of its initial viscosity values during the test interval. The degradation factor was calculated by the following equation:

$$Degradation\ factor = \left[ 1 - \left( \frac{\mu}{\mu_i} \right) \right] * 100\%$$

, where  $\mu_i$ -initial viscosity and  $\mu$ -the following viscosity of solution.

Subsequently, zeta potential measurements display that the solution was stable during the time as illustrated in Figure 44. These conducted experiments verify the stability of a combination of nanoparticle and polymer solutions. Final zeta potential values meet the stability range and degradation factor sustain 50% of its initial viscosity values during test interval.

## Long term stability test

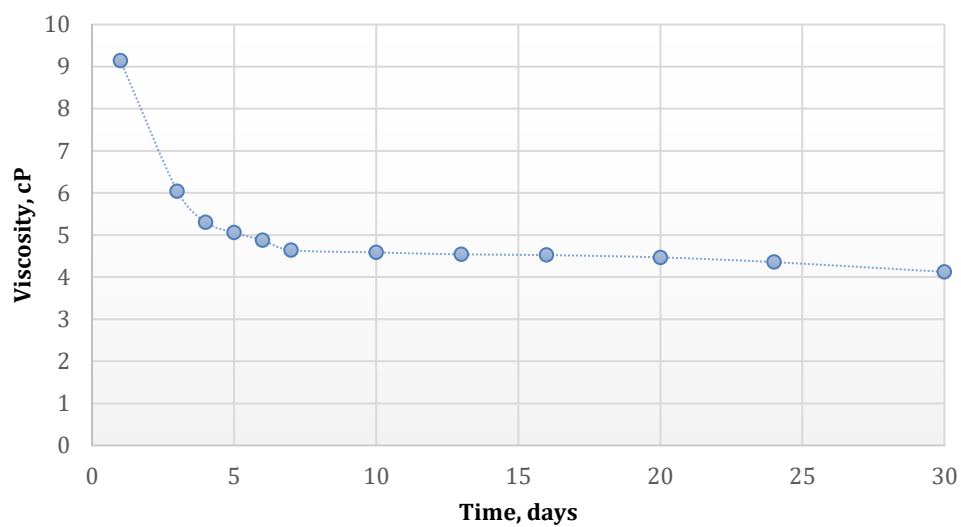


Figure 42. Long-term stability test of nano-assisted polymer solution

## Degradation of nano-assisted polymer solution

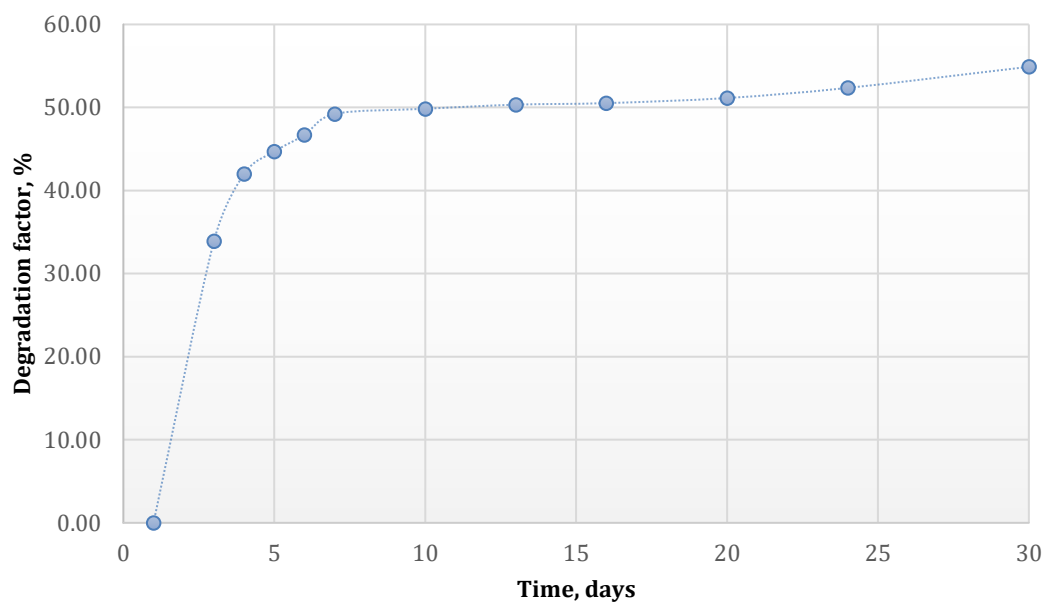


Figure 43. Thermal degradation factor of nano-assisted polymer solution

### Long term zeta potential test

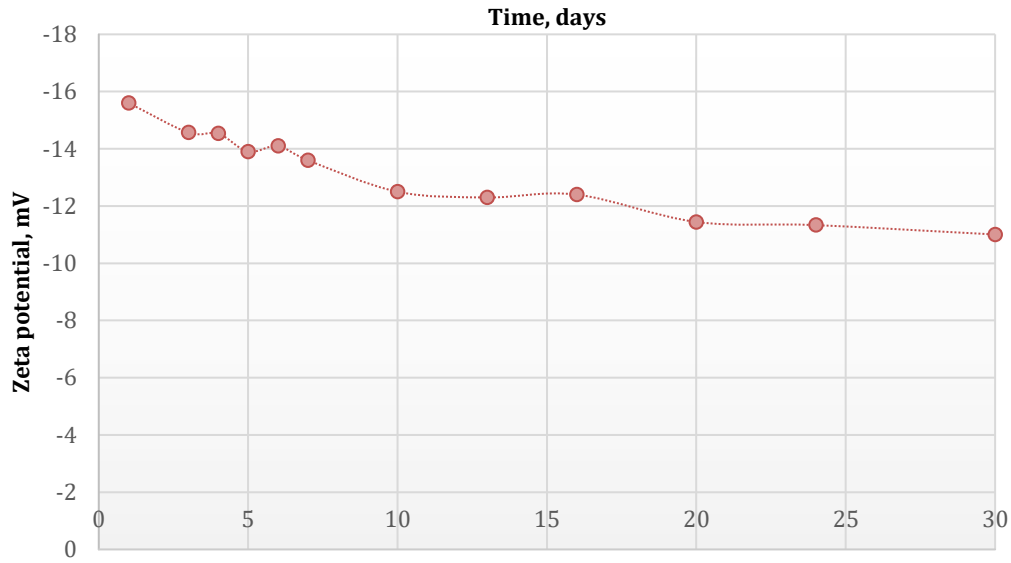


Figure 44. Long-term zeta potential test of nano-assisted polymer solution

### 4.5 Static adsorption analysis

The absorbance was measured for 5 fluid samples (4 nano-assisted polymer fluids and 1 nano-assisted polymer solution with a carbonate core) in the range of 200 and 400 nm wavelength. 5 fluid samples had a fixed concentration of SAV 10 polymer 2000 ppm and varying concentration silica nanoparticles 0.025, 0.05, 0.075, 0.1 wt%. Then, calibration curves were constructed to derive the linear equation. This is needed for the calculation of silica nanoparticle concentration.

Results show that absorbance increases with increasing concentration of silica nanoparticles as shown in Figure 45. The peak of absorbance was in the range of 220 and 230 nm. The final nanoparticle concentration after the addition of the carbonate core was calculated by the linear equation from the calibration curve:

$$y = kx + b, \rightarrow \text{Absorbance} = k * \text{NPs concentration} + b$$

$$\text{Absorbance} - b = \text{Corrected ABS} = k * \text{NPs concentration}$$

$$\text{NPs concentration} = \frac{1.577 - 1.4365}{12.332} = 0.011 \text{ wt\%}$$

, where absorbance value was taken from Figure 47 at its peak and slope and intercept were derived from Figure 45.

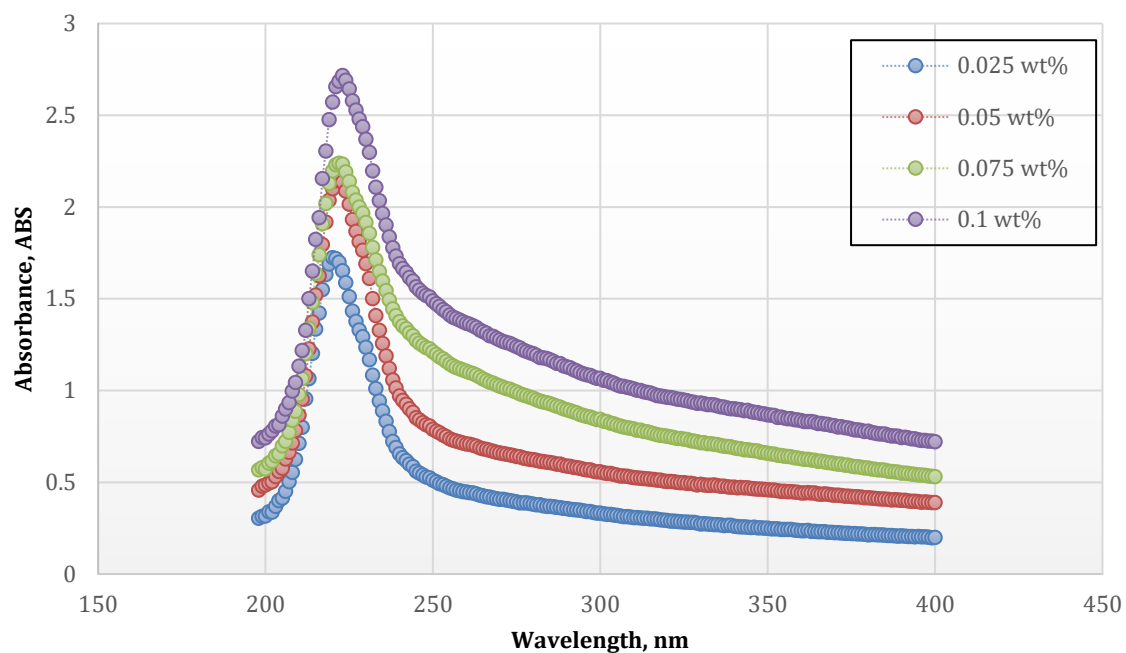


Figure 45. Absorbance of nano-assisted polymer fluids with increasing concentration of silica nanoparticle

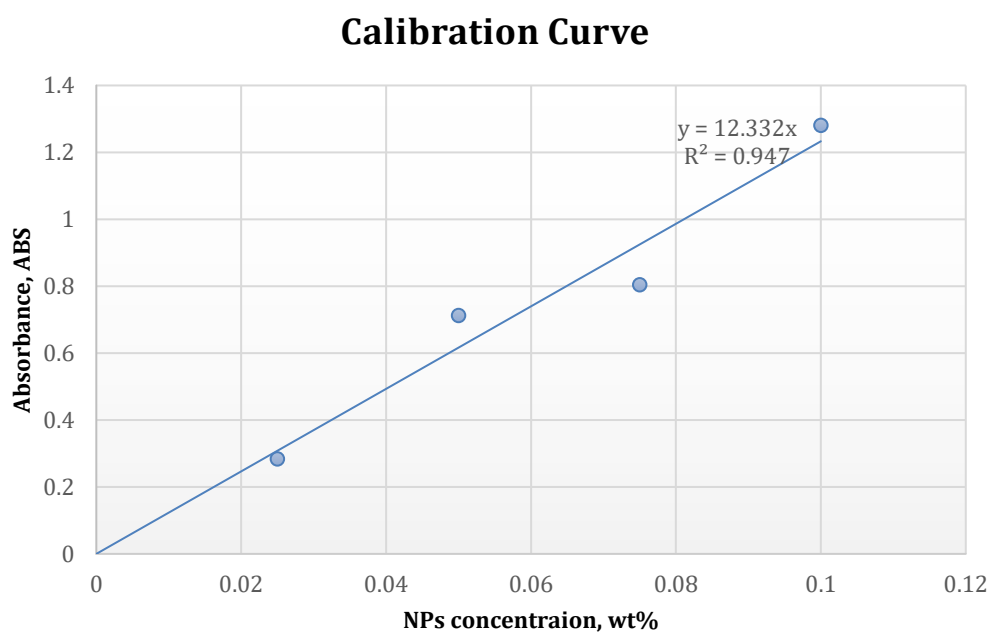


Figure 46. Corrected calibration curve

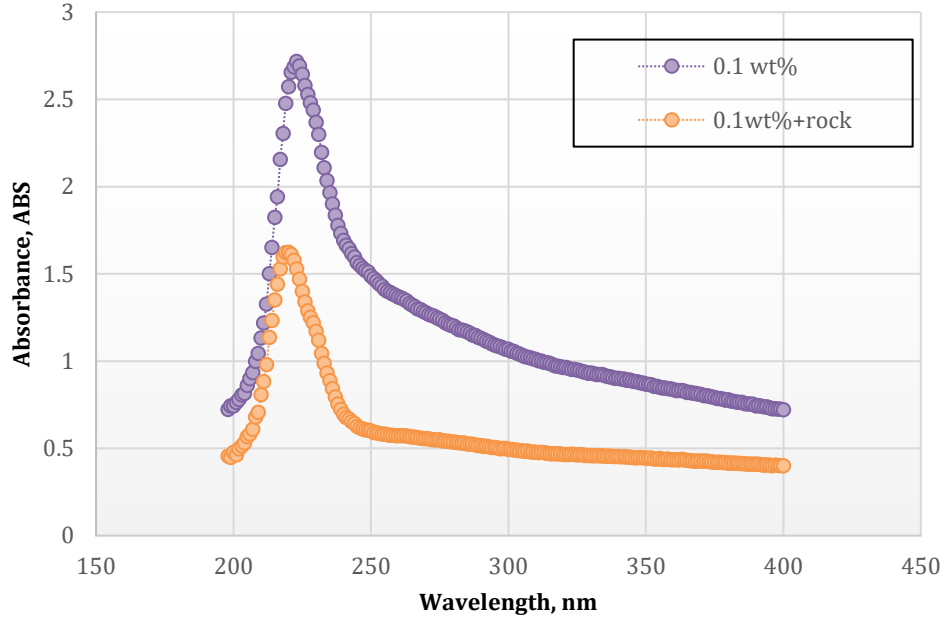


Figure 47. Comparison of two fluid absorbance

The silica nanoparticle concentration in the polymer solution after the addition of carbonate rock was 0.011 wt%. The adsorption was estimated by the following formula:

$$Adsorption = \left[ 1 - \left( \frac{NPs \text{ concentration after addition of rock}}{NPs \text{ concentration}} \right) \right] * 100\%$$

$$Adsorption = \left[ 1 - \left( \frac{0.011}{0.1} \right) \right] * 100\% = 88.61\%$$

The adsorption rate of nanoparticles in polymer solutions is high. It will indicate that the high amount of nanoparticles will settle on the surface of carbonate rock. Yu with colleagues investigated that the adsorption of silica nanoparticles in carbonate rocks was also high (Jianjia Yu, 2012). However, it's a benefit rather than a drawback. It can be explained as silica nanoparticles can significantly impact wettability alteration towards water-wet. The high rate of adsorption means a substantial amount of silica nanoparticles will cover the surface of carbonate rock. The results of contact angle measurements reveal that silica nanoparticle alters wettability towards the water-wet state. Thus, adsorbed silica nanoparticles significantly can change the contact angle of carbonate rock that is a suitable condition for increasing oil production.



## 5. Conclusions and Recommendations

In this research, the combination of nanoparticle and polymer flooding together to ensure improvement in the recovery mechanisms has been studied as the main target of the thesis. According to the results, subsequent finalization could be established:

- The combination of silica nanoparticle and modified synthetic polymer flooding was identified to be effective because the goals have been accomplished;
- Silicon oxide nanofluids alter wettability. The maximum alteration of carbonate rock wettability towards water-wet occurred by silica-based nanofluid with 0.1 wt % concentration. Therefore, it was screened as the optimum concentration for nanoparticle;
- The stability of the silica nanofluid decreases with increasing salinity. The highest salinity where  $SiO_2$  nanofluid was stable, was 40000 ppm. Thus, it was chosen as the optimum salinity. On the other hand, the stability of silica nanoparticles was increased with the addition of modified synthetic polymer. The 0.1 wt% silica nanoparticle showed maximum stability with 2000 ppm SAV 10 concentration;
- The addition of nanoparticles makes the polymer fluid more viscous in all cases. Adding 0.1 wt% of silica nanoparticle can increase viscosity of 2000 ppm SAV 10 polymer solution to 23.5 %, where the viscosity of nano-assisted polymer fluid become 4.85 cP at  $10\text{ s}^{-1}$ ,  $80^\circ\text{C}$ . It implies that the mobility ratio of the combination of nanoparticle and polymer is better than the mobility ratio of pure polymer solution;
- Nano-assisted polymer solution with 2000 ppm SAV 10 polymer, 0.1 wt %  $SiO_2$  nanoparticles concentrations was stable for 30 days at  $80^\circ\text{C}$ . Final zeta potential values meet the stability range and degradation factor sustain 50% of its initial viscosity values during long-term stability test interval;
- The adsorption rate of nanoparticles in polymer solutions is 88.61 %, which can significantly improve the wettability alteration property of nano-assisted polymer solution.

The recommendations are for advanced research to perform core flooding experiments, to investigate dynamic adsorption and to design smart injection techniques with the selected concentration of nano-assisted polymer solution.

## 6. REFERENCES

- A.Ghadimi, R. a. H., 2011. *A review of nanofluid stability properties and characterization in stationary conditions*. <https://doi.org/10.1016/j.ijheatmasstransfer.2011.04.014>: s.n.
- Abbas Roustaei, H. B., 17 August 2014. *Experimental investigation of SiO<sub>2</sub> nanoparticles on enhanced oil recovery of carbonate reservoirs*. *Journal Petroleum Exploration Production Technology* 5, 27–33 : <https://doi.org/10.1007/s13202-014-0120-3>.
- Achinta Bera, S. S. M. S. J. A. R. K. V., 2020. *Mechanistic study on silica nanoparticles-assisted guar gum polymer flooding for enhanced oil recovery in sandstone reservoirs*. <https://doi.org/10.1016/j.colsurfa.2020.124833>: s.n.
- Ahmed, T., 2010. *Reservoir engineering handbook fourth edition*. Elsevier: ISBN 0-88415-770-9.
- Aida Nasiri, M. S.-N. A. R. A. A. R. K., 2011. *Effect of dispersion method on thermal conductivity and stability of nanofluid*. <https://doi.org/10.1016/j.expthermflusci.2011.01.006>: s.n.
- Alex Nikolov, P. W. a. D. W., 2019. *Structure and stability of nanofluid films wetting solids: An overview*. <https://doi.org/10.1016/j.cis.2018.12.001>: s.n.
- Alomair O.A., M. M. a. A. H., August 2015. *Experimental Study of Enhanced-Heavy-Oil Recovery in Berea Sandstone Cores by Use of Nanofluids Applications*. SPE-171539: <https://doi.org/10.2118/171539-PA>.
- Argabright A., R. S. a. P. L., 1982. *Partially Hydrolyzed Polyacrylamides with Superior Flooding and Injection Properties*. SPE-11208-MS: <https://doi.org/10.2118/11208-MS>.
- Bayat E., J. R. S. A. P. A. a. H. M., September 2014. *Impact of Metal Oxide Nanoparticles on Enhanced Oil Recovery from Limestone Media at Several Temperatures*. American Chemical Society Publications: [dx.doi.org/10.1021/ef5013616](https://doi.org/10.1021/ef5013616).
- Carreau, P., 1972. *Rheological equations from molecular network theories*. *Transactions of the Society of Rheology* 16 (1), 99-127: <https://doi.org/10.1122/1.549276>.
- Cheraghian, G., 25 May 2016. *Effect of nano titanium dioxide on heavy oil recovery during polymer flooding*. *Petroleum Science and Technology*, 633-641: <https://doi.org/10.1080/10916466.2016.1156125>.
- D. Joshi, N. K. a. A. M., 2020. *Enhanced Oil Recovery Performance of Silica Nanofluid in Sandpack Model*. <https://doi.org/10.3997/2214-4609.202011923>: s.n.
- Dawson, R. a. L. R., October 1972. *Inaccessible Pore Volume in Polymer flooding*. SPE-3522-PA: <https://doi.org/10.2118/3522-PA>.

Debashis Dey, P. K. a. S. S., 2017. *A review of nanofluid preparation, stability, and thermo-physical properties*. <https://doi.org/10.1002/htj.21282>: s.n.

DeHekker G., B. L. C. V. a. B. B., 1986. *A Progress Report on Polymer-Augmented Waterflooding in Wyoming's North Oregon Basin and Byron Fields*. SPE-14953-MS: <https://doi.org/10.2118/14953-MS>.

Dejam, S. O. O. a. M., 2020. *Experimental Study on the Viscosity Behavior of Silica Nanofluids with Different Ions of Electrolytes*. <https://doi.org/10.1021/acs.iecr.9b06275>: s.n.

Ding, W. a., March 2005. *Experimental investigation into the pool boiling heat transfer of aqueous based  $\alpha$ -alumina nanofluids*. Journal of Nanoparticle Research (2005) 7: 265–274: DOI: 10.1007/s11051-005-3478-9.

Druetta P., a. P. F., 2019, February. *Polymer and nanoparticles flooding as a new method for Enhanced Oil Recovery*. s.l.:Journal of Petroleum Science and Engineering. ELSEVIER. <https://doi.org/10.1016/j.petrol.2019.02.070>.

Duda L., K. E. a. F. K., October 1981. *Influence of Polymer-Molecule/Wall Interactions on Mobility Control*. SPE-9298-PA: <https://doi.org/10.2118/9298-PA>.

Elgibalyd, M. I. R. M.-M. M. A., 2018. *Silica nanofluid flooding for enhanced oil recovery in sandstone rocks*. <https://doi.org/10.1016/j.ejpe.2017.01.006>: s.n.

Forough Ameli, M. R. M. A. A., 2019 . *On the effect of salinity and nano-particles on polymer flooding in a heterogeneous porous media: Experimental and modeling approaches*. <https://doi.org/10.1016/j.petrol.2018.12.015>: s.n.

Green, D. W. & Paul Willhite, G., n.d. *Enhanced Oil Recovery Second Edition*, s.l.: s.n.

H.Doe, A. M.-A. a. P., May 1987. *Hydrolysis and Precipitation of Polyacrylamide in Hard Brines at Elevated Temperatures*. SPE-13033-PA: <https://doi.org/10.2118/13033-PA>.

Hu Z., A. M. G. J. a. W. D., March 2016. *Nanoparticle-assisted water-flooding in Berea sandstones*. Energy Fuels 2016, 30, 4, 2791-2804: <https://doi.org/10.1021/acs.energyfuels.6b00051>.

Huges, D. T. D. C. C. a. T. J., February 1990. *Appraisal of the Use of Polymer Injection to Suppress Aquifer Influx and to Improve Volumetric Sweep in a Viscous Oil Reservoir*. SPE-17400-PA: <https://doi.org/10.2118/17400-PA>.

Jaafa M.Z.r, M. N. A. a. H. M., 2014. *Measurement of Isoelectric Point of Sandstone and Carbonate Rock for Monitoring Water Encroachment*. Journal of Applied Sciences, 14: 3349-3353: 10.3923/jas.2014.3349.3353.

Jacobi, R. B. a., February 2014. *Ultrasonication effects on thermal and rheological properties of carbon nanotube suspensions*. *Nanoscale Res Lett.* 2012; 7(1): 127.: DOI: 10.1186/1556-276X-7-127.

Jouenne, S., 2020. *Polymer flooding in high temperature, high salinity conditions: Selection of polymer type and polymer chemistry, thermal stability*.  
<https://doi.org/10.1016/j.petrol.2020.107545>: s.n.

Karimi A., F. B. A. K. P. D. B. A. R. a. A. S., January 2, 2012. *Wettability Alteration in Carbonates using Zirconium Oxide Nanofluids: EOR Implications*. *Energy Fuels* 2012, 26, 2, 1028-1036: <https://doi.org/10.1021/ef201475u>.

Karl, J. a. K., January 2019. *Low-Salinity Polymeric Nanofluid-Enhanced Oil Recovery Using Green Polymer-Coated ZnO/SiO<sub>2</sub> Nanocomposites in the Upper Qamchuqa Formation in Kurdistan Region, Iraq*. *Energy Fuels* 2019, 33, 927–937:  
 DOI:10.1021/acs.energyfuels.8b03847 .

Ke Liang, P. H. C. X. S. a. Y. F., 2019. *Comparative Study on Enhancing Oil Recovery under High Temperature and High Salinity: Polysaccharides Versus Synthetic Polymer*. *ACS OMEGA*: <https://doi.org/10.1021/acsomega.9b00717>.

Kierulf C., S. I., 1988. *The Thermal Stability of Xanthan*. *Carbohydrate polymers* volume 9, issue 3, 185-194: [https://doi.org/10.1016/0144-8617\(88\)90024-0](https://doi.org/10.1016/0144-8617(88)90024-0).

Krishnamoorti, R., November 2006. *Extracting the Benefits of Nanotechnology for the Oil Industry*. SPE-1106-0024-JPT: <https://doi.org/10.2118/1106-0024-JPT>.

Kumar Panigrahi, S. C., 2020. *Stability of nanofluid: A review*.  
<https://doi.org/10.1016/j.applthermaleng.2020.115259>: s.n.

Kumar, S. et al., 2020. *Enhancing the Performance of HPAM Polymer Flooding Using Nano CuO/Nanoclay Blend*. <https://doi.org/10.3390/pr8080907>: s.n.

L.P.Dake, 1978. *Fundamental of reservoir engineering*. Amsterdam: s.n.

Larry W.Lake, R. T. W. R. a. G. A., 2014. *Fundamentals of Enhanced oil recovery*, Texas: Society of Petroleum Engineers .

Laura Corredor, B. M. a. M. H., October 2018. *Improving Polymer Flooding By Addition Of Surface Modified Nanoparticles*. SPE-192141-MS: <https://doi.org/10.2118/192141-MS>.

Li K., W. D. a. J. S., 18 June 2018. *Review on enhanced oil recovery by nanofluids*. *Oil & Gas Science and Technology - Rev. IFP Energies nouvelles* 73, 37 (2018):  
<https://doi.org/10.1051/ogst/2018052>.

Lim K.T., R. H. B. W., 1992. *Steam distillation and oil quality during thermal oil recovery*, <https://doi.org/10.2118/23718-MS>: SPE 23718-MS.

M.Z. Sharif, W. A. A. R. a. N. N. M. Z., 2017. *Improvement of Nanofluid stability*. Vol SI 4(2),233-247, 2017: s.n.

Maghzi A., K. R. M. A. a. G. H., February 2014. *The impact of silica nanoparticles on the performance of polymer solution in presence of salts in polymer flooding for heavy oil recovery*. Journal Fuel, Volume 123, p.123-132: <https://doi.org/10.1016/j.fuel.2014.01.017>.

Marjan Ashrafizadeh, A. R. S. A. a. S. S., 2017. *Enhanced polymer flooding using a novel nano-scale smart polymer: Experimental investigation*. <https://doi.org/10.1002/cjce.22860>: s.n.

Ming Yue, W. Z. H. H. H. S. Y. L. Y. L., 2018. *Experimental research on remaining oil distribution and recovery performances after nano-micron polymer particles injection by direct visualization*. <https://doi.org/10.1016/j.fuel.2017.10.055>: s.n.

Moradi B., P. P. F. J. F. M. M. a. E. A., November, 2015. *Application of SiO<sub>2</sub> Nano Particles to Improve the Performance of Water Alternating Gas EOR Process*. SPE-178040-MS: <https://doi.org/10.2118/178040-MS>.

Muhammad Rehan Hashmet, Y. Q. E. S. M. W. A. a. A. M., April 2017. *Injection of Polymer for Improved Sweep Efficiency in High Temperature High Salinity Carbonate Reservoirs: Linear X-Ray Aided Flood Front Monitoring*. SPE-188125-MS: <https://doi.org/10.2118/188125-MS>.

NanoComposix, 2020. *Zeta potential analysis of nanoparticles*. s.l.:s.n.

Nares H.R., S.-H. P.-G. M. a. C.-R. M., 2007. *Heavy-Crude-Oil Upgrading With Transition Metals*. SPE-107837-MS: <https://doi.org/10.2118/107837-MS>.

Needham R.B., T. C. B. a. G. J. W., 1974. *Control Of Water Mobility Using Polymers and Multivalent Cations*. Tulsa, Oklahoma, SPE-4747-MS: <https://doi.org/10.2118/4747-MS>.

Niu yabin, S. j. , Z. z. W. g. , S. g. , a. S. l., February 2001. *Research on Hydrophobically Associating water-soluble polymer used for EOR*. Houston, Texas, SPE 65378, Society of Petroleum Engineers: <https://doi.org/10.2118/65378-MS>.

Ogolo N.A., O. O. a. O. M., April 2012. *Enhanced Oil Recovery Using Nanoparticles*. SPE-160847-MS: <https://doi.org/10.2118/160847-MS>.

Ragab, A. M. S., October 2015. *A Comparative Investigation of Nano Particle Effects from Improved Oil Recovery-Experimental Work*. SPE-175395-MS: <https://doi.org/10.2118/175395-MS>.

Rahul Saha, R. V. S. U. a. P. T., 20 April 2018. *Silica nanoparticle assisted polymer flooding of heavy crude oil: Emulsification, Rheology and Wettability Alteration characteristics*. American Chemical Society Publications: <https://doi.org/10.1021/acs.iecr.8b00540>.

S.P.Jang, Y. J. C. Y. S. C. B., 2007. *Stability and thermal conductivity characteristics of nanofluids*. <https://doi.org/10.1016/j.tca.2006.11.036>: s.n.

Sadik Umar, F. S. N. A. a. S. N. M., 2018. *Investigation of the effect of pH adjustment on the stability of nanofluid*. <https://doi.org/10.1063/1.5066987>: s.n.

Sandeep Rellegadla, H. K. B. M. R. K. G. P. S. N. N. P. S. J. a. A. A., 2018. *An Effective Approach for Enhanced Oil Recovery Using Nickel Nanoparticles Assisted Polymer Flooding*. <https://doi.org/10.1021/acs.energyfuels.8b02356>: s.n.

Sheng, J. J., 2011. *Modern Chemical Enhanced Oil Recovery: Theory and Practice*. s.l.:Elsevier.

Song, H., Pope, G. A. & Mohanty, K. K., September 24 2020. *Thermal Stability of Acrylamide-Based Polymers at High Temperature and High Salinity*. <https://doi.org/10.2118/199921-MS>: s.n.

Sönnichsen, N., 2021. *Global enhanced oil recovery market value 2018 & 2025*. s.l.:s.n.

Suleimanov B.A., I. F. a. V. E., 6 June 2011. *Nanofluid for enhanced oil recovery*. Journal of Petroleum Science and Engineering 78 (2011) 431-437: <https://doi.org/10.1016/j.petrol.2011.06.014>.

Tarek, M., September 2015. *Investigating Nano-Fluid Mixture Effects to Enhance Oil Recovery*. SPE-178739-STU: <https://doi.org/10.2118/178739-STU>.

Tsaur, K., December 1979. *Sensitivity study of Polymer flooding*. SPE-7079-PA: <https://doi.org/10.2118/7079-PA>.

Tushar Sharma, S. I. a. J. S. S., November 2016. *Silica Nanofluids in an Oilfield Polymer Polyacrylamide: Interfacial Properties, Wettability Alteration, and Applications for Chemical Enhanced Oil Recovery*. American Chemical Society: <https://doi.org/10.1021/acs.iecr.6b03299>.

Wang D., C. J. Y. Q. W. G. Q. L. a. C. F., 2000. *Viscous-Elastic Polymer Can Increase Microscale Displacement Efficiency in Cores*. SPE-63227-MS: <https://doi.org/10.2118/63227-MS>.

Wasan D., W. S. N. A. a. K. K., March 11, 2011. *Wetting and Spreading of Nanofluids on Solid Surfaces Driven by the Structural Disjoining Pressure: Statics Analysis and*

*Experiments*. American Chemical Society Publications. Langmuir 2011, 27, 7, 3324-3335: <https://doi.org/10.1021/la104204b>.

Xiaofei Sun, Y. Z. G. C. a. Z. G., February 2017. *Application of Nanoparticles in Enhanced Oil Recovery: A Critical Review of Recent Progress*. Energies 2017, 10(3), 345: <https://doi.org/10.3390/en10030345>.

Xia, S. et al., 2020. *Application of Polysaccharide Biopolymer in Petroleum Recovery*. <https://doi.org/10.3390/polym12091860>: s.n.

Xie, W. Y. a. H., 2011. *A Review on Nanofluids: Preparation, Stability Mechanisms, and Applications*. <https://doi.org/10.1155/2012/435873>: s.n.

Xin, X. et al., 2018. *Effect of Polymer Degradation on Polymer Flooding in Heterogeneous Reservoirs*. <https://doi.org/10.3390/polym10080857>: s.n.

Yadav U.S., K. H. a. R. V., 31 July 2019. *Experimental evaluation of partially hydrolyzed polyacrylamide and silica nanoparticles solutions for enhanced oil recovery*. Journal of Petroleum Exploration and Production Technology : <https://doi.org/10.1007/s13202-019-00749-8>.

Zhang H., N. A. a. W. D., April, 2014. *Enhanced Oil Recovery (EOR) Using Nanoparticle Dispersions: Underlying Mechanism and Imbibition Experiments*. American Chemical Society. Energy Fuels 2014, 28, 5, 3002-3009: <https://doi.org/10.1021/ef500272r>.